VALUING THE GLOBAL MORTALITY CONSEQUENCES OF CLIMATE CHANGE ACCOUNTING FOR ADAPTATION COSTS AND BENEFITS*

TAMMA CARLETON
AMIR JINA
MICHAEL DELGADO
MICHAEL GREENSTONE
TREVOR HOUSER
SOLOMON HSIANG
ANDREW HULTGREN
ROBERT E. KOPP
KELLY E. MCCUSKER
ISHAN NATH
JAMES RISING
ASHWIN RODE
HEE KWON SEO
ARVID VIAENE
JIACAN YUAN
ALICE TIANBO ZHANG

*This project is an output of the Climate Impact Lab, which gratefully acknowledges funding from the Energy Policy Institute of Chicago (EPIC), International Growth Centre, National Science Foundation, Sloan Foundation, Carnegie Corporation, and Tata Center for Development. Tamma Carleton acknowledges funding from the U.S. Environmental Protection Agency Science To Achieve Results Fellowship (no. FP91780401). We thank Trinetta Chong, Greg Dobbels, Diana Gergel, Radhika Goyal, Simon Greenhill, Hannah Hess, Dylan Hogan, Azhar Hussain, Stefan Klos, Theodor Kulczycki, Ruixue Li, Brewster Malevich, Sébastien Annan Phan, Justin Simcock, Emile Tenezakis, Jingyuan Wang, and Jong-kai Yang for invaluable research assistance during all stages of this project, and Samantha Anderson, Megan Landín, Terin Mayer, and Jack Chang for excellent project management. We thank Larry Katz, Andrei Shleifer, and five anonymous reviewers for insightful comments, as well as David Anthoff, Max Auffhammer, Olivier Deschênes, Avi Ebenstein, Nolan Miller, Wolfram Schlenker, and numerous workshop participants at University of Chicago, Stanford, Princeton, UC Berkeley, UC San Diego, UC Santa Barbara, University of Pennsylvania, University of San Francisco, University of Virginia, University of Wisconsin-Madison, University of Minnesota Twin Cities, NBER Summer Institute, LSE, PIK, Oslo University, University of British Columbia, Gothenburg University, the European Center for Advanced Research in Economics and Statistics, the National Academies of Sciences, and the Econometric Society for comments, suggestions, and help with data. Full replication code is publicly available at https://github.com/ClimateImpactLab/carleton_mortality_2022 and replication data are publicly hosted at doi.org/10.5281/zenodo.6416119.

The Quarterly Journal of Economics (2022), 2037–2105. https://doi.org/10.1093/qje/qjac020.
Advance Access publication on April 21, 2022.

Using 40 countries' subnational data, we estimate age-specific mortality-temperature relationships and extrapolate them to countries without data today and into a future with climate change. We uncover a U-shaped relationship where extreme cold and hot temperatures increase mortality rates, especially for the elderly. Critically, this relationship is flattened by higher incomes and adaptation to local climate. Using a revealed-preference approach to recover unobserved adaptation costs, we estimate that the mean global increase in mortality risk due to climate change, accounting for adaptation benefits and costs, is valued at roughly 3.2% of global GDP in 2100 under a high-emissions scenario. Notably, today's cold locations are projected to benefit, while today's poor and hot locations have large projected damages. Finally, our central estimates indicate that the release of an additional ton of CO_2 today will cause mortality-related damages of $36.6 under a high-emissions scenario, with an interquartile range accounting for both econometric and climate uncertainty of [−$7.8, $73.0]. These empirically grounded estimates exceed the previous literature's estimates by an order of magnitude. *JEL Codes:* Q51, Q54, H23, H41, I14.

I. Introduction

Understanding the likely global economic effects of climate change is of tremendous practical value to both policy makers and researchers. On the policy side, decisions are currently made with incomplete and inconsistent information on the benefits of greenhouse gas emissions reductions. These inconsistencies are reflected in global climate policy, which is at once lenient and wildly inconsistent. To date, the economics literature has struggled to mitigate this uncertainty, lacking empirically founded and globally comprehensive estimates of the total burden imposed by climate change that account for the benefits and costs of adaptation. This problem is made all the more difficult because emissions today influence the global climate for hundreds of years. Thus, any reliable estimate of the damage from climate change must include projections of economic effects that are both long run and at global scale.

Decades of study have produced numerous theoretical and empirical insights and important findings regarding the economics of climate change, but a fundamental gulf persists between the two main types of analyses. On the one hand, there are stylized models that are able to capture the multicentury and global nature of climate change, such as "integrated assessment models" (IAMs) (e.g., Nordhaus 1992; Tol 1997; Stern 2006). Their appeal is that they provide an answer to the question of what the global

costs of climate change will be, but IAMs require many assumptions, and this weakens the authority of their answers. On the other hand, there has been an explosion of highly resolved empirical analyses whose credibility lies in their use of real-world data and careful econometric measurement (e.g., Schlenker and Roberts 2009; Deschênes and Greenstone 2007). Yet these analyses tend to be limited in geographic extent and/or rely on short-run changes in weather that are unlikely to fully account for adaptation to gradual climate change (Hsiang 2016). At its core, this dichotomy persists because researchers have traded off being complete in scale and scope with investing heavily in data collection and analysis.

This article aims to resolve the tension between these approaches by providing empirically derived estimates of climate change's effects on global mortality risk. Importantly, these estimates are at the scale of IAMs, but grounded in detailed econometric analyses using high-resolution globally representative data, and account for adaptation to gradual climate change. The analysis proceeds in three steps that lead to the article's three main findings.

First, we estimate regressions to infer age-specific mortality-temperature relationships using the most comprehensive data set ever collected on annual, subnational mortality statistics from 40 countries that cover 38% of the global population. The benefits of adaptation to climate change and the benefits of projected future income growth are estimated by allowing the mortality-temperature response function to vary with long-run climate (e.g., Auffhammer 2018) and income per capita (e.g., Fetzer 2020). This modeling of heterogeneity allows us to predict the structure of the mortality-temperature relationship across locations where we lack mortality data, yielding estimates for the whole world.

These regressions uncover a plausibly causal U-shaped relationship where extremely cold and hot temperatures increase mortality rates, especially for those aged 65 and older. Moreover, this relationship is quite heterogeneous across the planet: we find that both income and a warmer long-run climate substantially moderate mortality sensitivity to temperature. When combining these results with current global data on climate, income, and population, we estimate that the effect of an additional very hot day (35°C/95°F) on mortality in the $>$ 64 age group is $\sim$50% larger in regions of the world where mortality data are unavailable. This finding suggests that prior estimates may understate

climate change effects, because they disproportionately rely on data from wealthy economies and temperate climates. However, the estimates of heterogeneity rely on cross-sectional variation and therefore must be considered associational.

Second, we combine the regression results with standard future predictions of climate, income, and population to project future climate change–induced mortality risk in terms of both changes in fatality rates and their monetized value. The article's mean estimate of the projected increase in the global mortality rate due to climate change is 73 deaths per 100,000 at the end of the century under a high-emissions scenario (i.e., Representative Concentration Pathway [RCP] 8.5), with an interquartile range of [6, 101] reflecting both econometric and climate uncertainty. This effect is similar in magnitude to the current global mortality burden of all cancers or all infectious diseases. It is noteworthy that these effects are predicted to be unequally distributed across the globe: for example, mortality rates in Accra, Ghana, are projected to increase by 17% at the end of the century under a high-emissions scenario due to an increase in very hot days, while in Berlin, Germany, mortality rates are projected to decrease by 15% because of milder winters. Perhaps most important, a failure to account for climate adaptation and the benefits of income growth would lead to overstating the mortality effects of climate change by a factor of about 3.

Of course, adaptation is costly. Although it is impossible to enumerate and observe all of the actions people take to modify their mortality risk of climate change, we develop a stylized revealed-preference model to infer the sum of these costs. This approach is based on the assumption that individuals undertake adaptation investments until the marginal benefits and costs of adaptation are equal. Because we can empirically observe adaptation benefits by measuring reduced mortality sensitivities to temperature based on a location's climate, we can then infer their marginal costs. Like all revealed-preference approaches, this one requires a set of nontrivial assumptions, including that there are optimizing agents and that key markets are frictionless.

We estimate that the full mortality risk of climate change, including the benefits and inferred costs of adaptation, is equal to roughly 3.2% of global GDP at the end of the century under a high-emissions scenario, with an interquartile range of [−5.4%, 9.1%]. In addition, we find that poor countries are projected to disproportionately experience these effects through deaths, while wealthy

countries experience effects largely through costly adaptation investments. This monetization of climate change's full mortality risk is accomplished by applying the value of a statistical life (VSL) to projected deaths and using the revealed-preference approach to infer adaptation costs.

Third, we use these estimates to compute the global marginal willingness to pay (MWTP) to avoid the alteration of mortality risk associated with the temperature change from the release of an additional metric ton of CO_2. We call this the mortality "partial" social cost of carbon (SCC); a "full" SCC would encompass effects across all affected outcomes (and changes in mortality due to other features of climate change, like storms). Our estimates imply that the mortality partial SCC is roughly \$36.6 [−\$7.8, \$73.0] (in 2019 US\$) with a high-emissions scenario (RCP8.5) under a 2% discount rate, using an age-varying VSL and assuming agents are risk-neutral.[1] For convenience, we refer to this as the "preferred" mortality partial SCC going forward, but we also report estimates based on many alternative valuation assumptions.[2]

It is noteworthy that the mortality partial SCC is estimated with considerable uncertainty, stemming from climatological and econometric sources and that its distribution is right skewed. We follow Nath et al. (2022) and use this distribution to compute a certainty-equivalent mortality partial SCC with standard risk aversion parameters. This calculation results in a mortality partial SCC that is several times larger than the estimate assuming that agents are risk neutral, which has been standard in prior policy applications of the SCC (Greenstone, Kopits, and Wolverton 2013).

Overall, this article's results suggest that the temperature-related mortality risk from climate change is substantially greater than previously understood. For example, the preferred mortality partial SCC is more than an order of magnitude larger than the partial SCC for all health effects embedded in the Framework for Uncertainty, Negotiation, and Distribution (FUND) IAM.

1. This value falls to \$17.1 [−\$24.7, \$53.6] with a moderate-emissions scenario (RCP4.5). The mortality partial SCC is lower in this scenario because the relationship between mortality risk and temperature is convex, meaning that marginal damages are greater under higher baseline emissions.

2. We call this approach to constructing an empirically based partial SCC the Data-Driven Spatial Climate Impact Model (DSCIM). DSCIM is also outlined in Rode et al. (2021), where it is used to estimate a partial SCC for energy consumption.

Further, under the high-emissions scenario, the estimated mortality partial SCC is ~72% of the Biden Administration's full interim SCC (Carleton and Greenstone forthcoming).

In generating these results, this article overcomes multiple challenges that have plagued the previous literature. The first challenge is that CO_2 is a global pollutant, so it is necessary to account for the heterogeneous costs of climate change across the whole planet. The second challenge is that today there is substantial adaptation to climate, as people successfully live in both Lahore, Pakistan, and Anchorage, AK, and climate change will undoubtedly lead to new adaptations in the future. The extent to which investments in adaptation can limit the effects of climate change is a critical component of damage estimates. We address these challenges by combining extensive data with an econometric approach that models heterogeneity in the mortality-temperature relationship, allowing us to predict mortality-temperature relationships at high resolution globally, today and in the future as climate and incomes evolve. Specifically, we develop estimates of climate change effects for 24,378 separate regions around the world that are about the size of a U.S. county. In contrast, the previous literature has assumed that the world is composed of, at maximum, 170 heterogenous regions (Burke, Hsiang, and Miguel 2015), but typically far fewer (Nordhaus and Yang 1996; Tol 1997), and has missed the striking heterogeneity we uncover.

A final challenge is that adaptation responses are costly, and these costs must be accounted for in a full assessment of climate change effects. While our revealed-preference approach to inferring adaptation costs relies on a strong set of simplifying assumptions, it can be directly estimated with available data. In addition, it represents an important advance on previous literature, which has ignored adaptation (e.g., Deschênes and Greenstone 2007), quantified adaptation benefits without estimating costs (e.g., Heutel, Miller, and Molitor 2017), or tried to measure the costs of individual adaptive investments in selected locations (e.g., Barreca et al. 2016), an approach that is poorly equipped to capture the wide range of potential responses to warming.

The rest of this article is organized as follows: Section II provides definitions and some basic intuition for the economics of adaptation to climate change in the context of mortality. Section III details the data used throughout the analysis. Section IV describes our empirical model and estimation results. Section V presents projections of climate change effects with and without the

benefits of adaptation. Section VI outlines a revealed-preference approach that allows us to infer adaptation costs and uses this framework to present empirically derived projections of the full mortality risk of climate change, accounting for the costs and benefits of adaptation. Section VII constructs a partial SCC, Section VIII discusses key limitations of the analysis, and Section IX concludes.

II. Conceptual Framework

This section sets out a simple conceptual framework that guides the empirical model used to estimate society's willingness to pay (WTP) to avoid the mortality risks from climate change. In estimating these mortality risks, it is critical to account for individuals' compensatory responses, or adaptations, to climate change, such as investments in air conditioning. These adaptations have benefits that reduce the risks of extreme temperatures and costs in the form of forgone consumption. Thus, the full mortality risk of climate change is the sum of changes in mortality rates after accounting for adaptation and the costs of those adaptations. Here, we define some key objects that the article will estimate, including the full mortality risk due to climate change.

We define the climate as the joint probability distribution of possible weather conditions that can be expected to occur over a specific interval of time. Following the notation of Hsiang (2016), let $\boldsymbol{C}$ be a vector of parameters describing the entire joint probability distribution over all relevant climatic variables (e.g., the mean and variance of daily average temperature).

We define weather realizations as a random vector $\boldsymbol{c}$ drawn from a distribution characterized by $\boldsymbol{C}$. Mortality risk is a function of both weather $\boldsymbol{c}$ and a composite good $\boldsymbol{b} = \xi(b_1, \ldots, b_K)$ comprising all choice variables b_k that could influence mortality risk, such as installation of air conditioning and time allocated to indoor activities. The endogenous choices in $\boldsymbol{b}$ are the outcome of a stylized model in which individuals maximize expected utility by trading off consumption of a numeraire good and $\boldsymbol{b}$, subject to a budget constraint with exogenous income Y, as outlined in greater detail in Section VI. Mortality risk is then captured by the probability of death $f = f(\boldsymbol{b}, \boldsymbol{c})$.

Climate change will influence mortality risk through two pathways. First, a change in $\boldsymbol{C}$ will directly alter realized weather draws, changing $\boldsymbol{c}$. Second, a change in $\boldsymbol{C}$ can alter individuals' beliefs about their likely weather realizations, shifting how they

act, and ultimately changing their endogenous choice variables $\boldsymbol{b}$. Endogenous adjustments to $\boldsymbol{b}$ therefore capture all long-run adaptation to the climate (e.g., Mendelsohn, Nordhaus, and Shaw 1994; Kelly, Kolstad, and Mitchell 2005). Since the climate $\boldsymbol{C}$ determines both $\boldsymbol{c}$ and $\boldsymbol{b}$, the probability of death in an initial time period t_0 is written as:

$$\Pr(\text{death} \mid Y_{t_0}, \boldsymbol{C}_{t_0}) = f(\boldsymbol{b}(Y_{t_0}, \boldsymbol{C}_{t_0}), \boldsymbol{c}(\boldsymbol{C}_{t_0})), \tag{1}$$

where $\boldsymbol{c}(\boldsymbol{C})$ is a random vector $\boldsymbol{c}$ drawn from the distribution characterized by $\boldsymbol{C}$ and $\boldsymbol{b}$ is influenced by income Y through the budget constraint.

The mortality effects of climate change between periods t_0 and t are then defined as:

$$\begin{aligned} &\textit{mortality effects of climate change} \\ &= f(\boldsymbol{b}(Y_t, \boldsymbol{C}_t), \boldsymbol{c}(\boldsymbol{C}_t)) - f(\boldsymbol{b}(Y_t, \boldsymbol{C}_{t_0}), \boldsymbol{c}(\boldsymbol{C}_{t_0})), \end{aligned} \tag{2}$$

which accounts for the adjustment of $\boldsymbol{b}$ in response to changes in both income and climate between the periods t_0 and t. Note that both terms in equation (2) include income in the future period t to isolate the role of climate change from changes in temperature-induced mortality that arise due to income growth.[3]

Many previous empirical studies assume that individuals do not make any adaptations or compensatory responses to an altered climate or to changes in income (e.g., Deschênes and Greenstone 2007; Houser et al. 2015). This leads to an incomplete measure of the mortality effects of climate change. To capture this object, we define the mortality effects of climate change without income growth or climate adaptation as:[4]

$$\begin{aligned} &\textit{mortality effects of climate change (without income growth} \\ &\textit{or adaptation)} = f(\boldsymbol{b}(Y_{t_0}, \boldsymbol{C}_{t_0}), \boldsymbol{c}(\boldsymbol{C}_t)) - f(\boldsymbol{b}(Y_{t_0}, \boldsymbol{C}_{t_0}), \boldsymbol{c}(\boldsymbol{C}_{t_0})), \end{aligned} \tag{2a}$$

3. This accounts for the possibility that cooling technologies like air conditioning are normal goods and that demand for them will increase as incomes rise, regardless of how climate change unfolds.

4. For parsimony, we use the term *adaptation* throughout the article to refer to adaptation in response to changes in the climate, as opposed to changes in adaptive behaviors or investments caused by changes in income or other variables.

which shuts down the possibility that individuals will choose new values of $\boldsymbol{b}$ as their incomes and their beliefs about $\boldsymbol{C}$ evolve. If the climate is changing such that the mortality risk from $\boldsymbol{C}_t$ is higher than $\boldsymbol{C}_{t_0}$ when holding $\boldsymbol{b}$ fixed, then the endogenous adjustment of $\boldsymbol{b}$ will weakly reduce mortality rates. In practice, the sign of the difference between equations (2) and (2a) will depend on the degree to which climate change reduces deadly extremely cold days versus increases deadly extremely hot days, as well as the optimal adaptation that agents undertake in response to these competing changes. Several analyses have estimated reduced-form versions of these equations, finding that accounting for endogenous changes to technology, behavior, and investment mitigates the direct effects of climate in a variety of contexts (e.g., Barreca et al. 2016).[5]

A second incomplete measure of the mortality effects of climate change is useful for quantifying the relative importance of income growth and climate adaptation in determining climate change outcomes. This measure captures the change in mortality rates that would be expected from climate change if incomes change, but climate adaptation is shut down. We define the mortality effects of climate change without climate adaptation as:

$$\begin{aligned} &\textit{mortality effects of climate change (without adaptation)} \\ &= f(\boldsymbol{b}(Y_t, \boldsymbol{C}_{t_0}), \boldsymbol{c}(\boldsymbol{C}_t)) - f(\boldsymbol{b}(Y_t, \boldsymbol{C}_{t_0}), \boldsymbol{c}(\boldsymbol{C}_{t_0})). \end{aligned} \tag{2b}$$

Although the mortality effects of climate change defined in equation (2) account for the benefits of adaptation, they do not account for its costs. If adjustments to $\boldsymbol{b}$ were costless and provided protection against the climate, we would expect universal uptake of highly adapted values for $\boldsymbol{b}$ so that temperature would have no effect on mortality. But we do not observe this to be true: for example, Heutel, Miller, and Molitor (2017) find that the mortality effects of extremely hot days in warmer climates (e.g., Houston) are much smaller than in more temperature climates (e.g., Seattle). We denote the costs of achieving adaptation level $\boldsymbol{b}$ as $A(\boldsymbol{b})$, measured in dollars of forgone consumption.

A full measure of the economic burden of climate change must account for not only the benefits generated by compensatory

5. For additional examples, see Schlenker and Roberts (2009); Hsiang and Narita (2012); Butler and Huybers (2013); Hsiang and Jina (2014); Barreca et al. (2015); Heutel, Miller, and Molitor (2017); Auffhammer (2018).

responses to these changes but also their cost. Thus, the full mortality risk of climate change between t_0 and t is defined as:

$$\begin{aligned} &\textit{full mortality risk of climate change} \\ &= VSL_t \underbrace{\left[f(\boldsymbol{b}(Y_t, \boldsymbol{C}_t), \boldsymbol{c}(\boldsymbol{C}_t)) - f(\boldsymbol{b}(Y_t, \boldsymbol{C}_{t_0}), \boldsymbol{c}(\boldsymbol{C}_{t_0})) \right]}_{\text{mortality effects of climate change}} \\ &+ \underbrace{A(\boldsymbol{b}(Y_t, \boldsymbol{C}_t)) - A(\boldsymbol{b}(Y_t, \boldsymbol{C}_{t_0}))}_{\text{adaptation costs}}, \end{aligned} \tag{3}$$

which is measured in dollars and where *VSL* is the value of a statistical life (Thaler and Rosen 1976). It is apparent that omitting the costs of adaptation would lead to an incomplete measure of the full mortality risk of climate change.

This article develops an empirical model to quantify equation (3), or the full mortality risk of climate change, at global scale. The first term (i.e., equation (2)) can be estimated directly and our empirical approach to doing so, as well as the resulting climate change effect projections, are detailed in Sections IV and V, respectively. Throughout the analysis, we consider the effects of changes in daily average temperature, such that the mortality effects of climate change include effects of temperature only (as opposed to other climate variables, such as hurricanes).

The second term in equation (3), or the change in adaptation costs between time periods, cannot be observed directly. In principle, data on each adaptive action could be gathered and modeled (e.g., Deschênes and Greenstone 2011), but since there exists an enormous number of possible adaptive margins that make up the vector $\boldsymbol{b}$, a complete enumerative approach is impractical. To make progress on quantifying adaptation costs, we develop a stylized revealed-preference approach that leverages observed differences in climate sensitivity across locations to infer adaptation costs associated with the mortality risk from climate change. This revealed-preference approach, and the resulting estimates of the full mortality risk of climate change (i.e., equation (3)), are reported in Section VI.

III. Data

To estimate the mortality risks of climate change at global scale, we assemble a novel data set composed of historical

mortality records, historical climate data, and future projections of climate, population, and income across the globe. Section III.A describes the data necessary to estimate $f(\boldsymbol{b}, \boldsymbol{c})$, the relationship between mortality and temperature, accounting for endogenous adaptation. Section III.B outlines the data we use to predict the mortality-temperature relationship across the entire planet today and project it into the future as populations adapt to climate change. Online Appendix B provides a more extensive description of all data sets.

III.A. Data to Estimate the Mortality-Temperature Relationship

1. *Mortality Data.* Our mortality data are collected independently from 40 countries.[6] Combined, this data set covers mortality outcomes for 38% of the global population, representing a substantial increase in coverage relative to existing literature; prior studies investigate an individual country (e.g., Burgess et al. 2017) or region (e.g., Deschênes 2018), or combine small nonrandom samples from across multiple countries (e.g., Gasparrini et al. 2017). Table I summarizes each data set, while spatial coverage, resolution, and temporal coverage are shown in Online Appendix Figure B.1. We harmonize all records into a single multicountry unbalanced panel data set of age-specific annual mortality rates, using three age categories: < 5, 5–64, and > 64, where the unit of observation is the second administrative unit, or ADM2 (e.g., a county in the United States) by year.

2. *Historical Climate Data.* The analysis is performed with two separate groups of historical data on precipitation and temperature. First, we use the Global Meteorological Forcing Dataset (GMFD) (Sheffield, Goteti, and Wood 2006), which relies on a weather model in combination with observational data. Second, we repeat our analysis with climate data sets that strictly interpolate observational data across space onto grids, combining temperature data from the daily Berkeley Earth Surface Temperature data set (BEST) (Rohde et al. 2013) with precipitation data from the monthly University of Delaware data set (UDEL) (Matsuura and Willmott 2007). Table I summarizes these data; full data descriptions are provided in Online Appendix B.2. We

6. We additionally use data from India as cross-validation of our main results, as the India data do not have records of age-specific mortality rates. The inclusion of India increases our data coverage to 55% of the global population.

TABLE I

HISTORICAL MORTALITY AND CLIMATE DATA

Country	N	Spatial scale[c]	Years	Age categories	Average annual mortality rate*[a]		Global pop. share[d]	Average covariate values*[b]		
					All-age	>64 yr.		GDP per capita[e]	Avg. daily temp.[f]	Annual avg. days >28°C
Panel A: Mortality records										
Brazil	228,762	ADM2	1997–2010	< 5, 5–64, >64	525	4,096	0.028	11,192	23.8	35.2
Chile	14,238	ADM2	1997–2010	< 5, 5–64, >64	554	4,178	0.002	14,578	14.3	0
China	7,488	ADM2	1991–2010	< 5, 5–64, >64	635	7,507	0.193	4,875	15.1	25.2
EU	13,013	NUTS2[g]	1990[h]–2010	< 5, 5–64, >64	1,014	5,243	0.063	22,941	11.2	1.6
France[i]	3,744	ADM2	1998–2010	0–19, 20–64, >64	961	3,576	0.009	31,432	11.9	0.3
India[j]	12,505	ADM2	1957–2001	All ages	724	–	0.178	1,355	25.8	131.4
Japan	5,076	ADM1	1975–2010	< 5, 5–64, >64	788	4,135	0.018	23,241	14.3	8.3
Mexico	146,835	ADM2	1990–2010	< 5, 5–64, >64	561	4,241	0.017	16,518	19.1	24.6
United States	401,542	ADM2	1968–2010	< 5, 5–64, >64	1,011	5,251	0.045	30,718	13	9.5
All countries	**833,203**	**–**	**–**	**–**	**780**	**4,736**	**0.554**	**20,590**	**15.5**	**32.6**

TABLE I

CONTINUED

Data set	Citation	Method	Resolution	Variable	Source
Panel B: Historical climate data sets					
GMFD, V1	Sheffield, Goteti, and Wood (2006)	Reanalysis and interpolation	0.25°	temp. & precip.	Princeton University
BEST	Rohde et al. (2013)	Interpolation	1°	temp.	Berkeley Earth
UDEL	Matsuura and Willmott (2007)	Interpolation	0.5°	precip.	University of Delaware

Notes.

*In units of deaths per 100,000 population.

[a]To remove outliers, particularly in low-population regions, we winsorize the mortality rate at the 1% level at the high end of the distribution across administrative regions, separately for each country.

[b]All covariate values shown are averages over the years in each country sample.

[c]ADM2 refers to the second administrative level (e.g., county), and ADM1 refers to the first administrative level (e.g., state). NUTS2 refers to the Nomenclature of Territorial Units for Statistics 2nd level, which is specific to the European Union (EU) and falls between first and second administrative levels.

[d]Global population share for each country in our sample is shown for 2010.

[e]GDP per capita values shown are in constant 2005 dollars purchasing power parity.

[f]Average daily temperature and annual average of the number of days above 28° C are both population weighted, using population values from 2010.

[g]EU data for 33 countries were obtained from a single source. Detailed descriptions of the countries in this region are presented in Online Appendix B.1.

[h]Most countries in the EU data have records beginning in 1990, but start dates vary for a small subset of countries. See Online Appendix B.1 and Table B.1 for details.

[i]We separate France from the rest of the EU, as higher-resolution mortality data are publicly available for France.

[j]It is widely believed that data from India understate mortality rates due to incomplete registration of deaths.

link climate and mortality data by aggregating gridded daily temperature data to the annual measures at the same administrative level as the mortality records (ADM2).

3. *Covariate Data.* The analysis allows for heterogeneity in the age-specific mortality-temperature relationship as a function of two long-run covariates: a measure of climate (i.e., long-run average temperature) and income per capita. We assemble time-invariant measures of these variables at the first administrative unit, or ADM1 (e.g., a state in the United States) level using GMFD climate data and a combination of the Penn World Tables (PWT), Gennaioli et al. (2014), and Eurostat (2013). These covariates are measured at the ADM1 scale (as opposed to the ADM2 scale of the mortality records) because of limited availability of higher-resolution income data. The construction of the income variable requires downscaling; details are provided in Online Appendix B.3.

In a set of robustness checks, we analyze five additional sources of heterogeneity, each of which has been suggested in the literature as an important driver of long-run well-being. These data include country-by-year observations of institutional quality from the Center for Systemic Peace (2020) (Glaeser et al. 2004); access to health care services (Bailey and Goodman-Bacon 2015), labor force informality (La Porta and Shleifer 2014), and educational attainment from the World Bank (2020) and the Organisation of Economic Co-operaton and Development (2020); and within-country income inequality from the World Inequality Lab (2020) (Alesina and Rodrik 1994).

III.B. Data for Projecting the Mortality-Temperature Relationship around the World and into the Future

1. *Unit of Analysis for Projections.* We partition the global land surface into a set of 24,378 regions and for each region we generate location-specific projected damages of climate change. The finest level of disaggregation in previous estimates of global climate change damages divides the world into 170 regions (Burke, Hsiang, and Miguel 2015), but most papers account for much less heterogeneity (Nordhaus and Yang 1996; Tol 1997). These regions (hereafter, impact regions) are constructed such that they are either identical to, or are a union of, existing administrative regions. They (i) respect national borders, (ii) are roughly

equal in population across regions, and (iii) display approximately homogeneous within-region climatic conditions. Online Appendix C details the algorithm used to create impact regions.

2. *Climate Projections.* We use a set of 21 high-resolution, bias-corrected, global climate projections produced by NASA Earth Exchange (NEX) (Thrasher et al. 2012) that provide daily temperature and precipitation through the year 2100. We obtain climate projections based on two standardized emissions scenarios: Representative Concentration Pathways 4.5 (RCP4.5, an emissions stabilization scenario) and 8.5 (RCP8.5, a scenario with intensive growth in fossil fuel emissions) (Thomson et al. 2011; Van Vuuren et al. 2011).

These 21 climate models systematically underestimate tail risks of future climate change (Tebaldi and Knutti 2007; Rasmussen, Meinshausen, and Kopp 2016).[7] To correct for this, we assign probabilistic weights to climate projections and use 12 surrogate models that describe local climate outcomes in the tails of the climate sensitivity distribution (Rasmussen, Meinshausen, and Kopp 2016; Hsiang et al. 2017). Online Appendix Figure B.2 shows the resulting weighted climate model distribution. The 21 models and 12 surrogate models are treated identically in all calculations and are collectively described as the surrogate/model mixed ensemble (SMME). Gridded output from these 33 projections are aggregated to impact regions.

Only 6 of the 21 models used to construct the SMME provide climate projections after 2100 for high- and moderate-emissions scenarios, and none simulate the effect of a marginal ton of CO_2. Therefore, in our estimates of the mortality partial SCC, we rely on the Finite Amplitude Impulse Response (FAIR) simple climate model, which has been developed especially for this type of calculation (Millar et al. 2017). Details on our implementation of FAIR are in Online Appendix G.

3. *Socioeconomic Projections.* Projections of population and income are a critical ingredient in the analysis, and for these we

7. The underestimation of tail risks in the 21-model ensemble arises because the ensemble was not designed to sample from a full distribution, the models exhibit idiosyncratic biases, and the distribution has narrow tails. We correct for bias and narrowness with respect to global mean surface temperature (GMST) projections, but our method does not correct for all biases.

rely on the Shared Socioeconomic Pathways (SSPs), which describe a set of plausible scenarios of socioeconomic development over the twenty-first century. We use SSP2, SSP3, and SSP4, which yield emissions in the absence of mitigation policy that fall between RCP4.5 and RCP8.5 in integrated assessment modeling exercises (Riahi et al. 2017). For population, we use the International Institute for Applied Systems Analysis (IIASA) SSP population projections, which provide estimates of population by age cohort at country level in five-year increments (IIASA Energy Program 2016). National population projections are allocated to impact regions based on current satellite-based within-country population distributions from Bright et al. (2012). Projections of national income per capita are similarly derived from the SSP scenarios, using both the IIASA projections and the OECD Env-Growth model (Dellink et al. 2015) projections. We allocate national income per capita to impact regions using current nighttime light satellite imagery from the NOAA Defense Meteorological Satellite Program (DSMP).

Because SSP projections are not available after the year 2100, our calculation of the mortality partial SCC relies on an extrapolation of the relationship between mortality-related climate change damages and global temperature change to later years; see Section VII for details.

4. *Value of a Statistical Life.* We use the value of a statistical life (VSL) to convert projected changes in mortality rates into dollars. Our primary approach relies on the U.S. EPA's VSL estimate of $10.95 million (2019 US$).[8] We transform the VSL into a value per life-year lost using a method described in Online Appendix H.1, which allows us to compute the total value of expected life-years lost due to climate change, accounting for different mortality-temperature relationships across age groups. We allow the VSL to vary with income, following the existing literature (e.g., Viscusi 2015) in using an income elasticity of unity to adjust the U.S. estimates of the VSL to different income levels

8. This VSL is from the 2012 U.S. EPA Regulatory Impact Analysis (RIA) for the Clean Power Plan Final Rule, which provides a 2020 income-adjusted VSL in 2011 US$, which we convert to 2019 US$. This VSL is also consistent with income- and inflation-adjusted versions of the VSL used in the U.S. EPA RIAs for the National Ambient Air Quality Standards for Particulate Matter (2012) and the repeal of the Clean Power Plan (2019), among many other RIAs.

across the world and over time.[9] When computing the mortality partial SCC in Section VII, we provide multiple alternative valuation assumptions in addition to this benchmark case.

IV. Empirical Estimates of the Mortality-Temperature Relationship, Accounting for Income and Climate Heterogeneity

This section describes our empirical approach to estimate the heterogeneous effect of temperature on mortality across the globe using historical data. This method allows us to capture differences in temperature sensitivity across distinct populations and thus quantify the benefits of adaptation and income as observed historically. Section V details how we combine this empirical information with standard projection data to construct estimates of the mortality effects of climate change (i.e., equation (2)).

IV.A. Empirical Model

We estimate the mortality-temperature relationship using a pooled sample of age-specific mortality rates across 40 countries. The effect of temperature on mortality rates is identified using year-to-year variation in the distribution of daily weather following, for example, Deschênes and Greenstone (2011). In addition, we allow the effect of temperature to vary with average temperature (i.e., long-run climate) and average per capita incomes.[10]

The two factors defining this interaction model reflect the economics governing adaptation. First, a higher long-run average temperature incentivizes investment in heat-related adaptive behaviors (e.g., air conditioning), as the return to any given adaption is higher the more frequently the population experiences days with life-threatening temperatures. Second, higher incomes relax agents' budget constraints and hence facilitate adaptive behavior.

9. The EPA considers a range of income elasticity values for the VSL, from 0.1 to 1.7 (U.S. Environmental Protection Agency 2016b), although their central recommendations are 0.7 and 1.1 (U.S. Environmental Protection Agency 2016a). A review by Viscusi (2015) estimates an income elasticity of the VSL of 1.1.

10. These two factors have been the focus of studies modeling heterogeneity across the broader climate-economy literature. For examples, see Mendelsohn, Nordhaus, and Shaw (1994); Kahn (2005); Auffhammer and Aroonruengsawat (2011); Hsiang, Meng, and Cane (2011); Graff Zivin and Neidell (2014); Moore and Lobell (2014); Davis and Gertler (2015); Heutel, Miller, and Molitor (2017); Isen, Rossin-Slater, and Walker (2017).

In other words, people live successfully in both Anchorage, AK, and Houston, TX, due to compensatory responses to their climate, and the wealthy purchase more safety. To capture these effects, we interact a nonlinear temperature response function with location-specific measures of climate and per capita income.

Specifically, we estimate the following model:

$$M_{ait} = g_a(\boldsymbol{T}_{it},\ TMEAN_s, \log(GDPpc)_s) + q_{ca}(\boldsymbol{R}_{it}) + \alpha_{ai} + \delta_{act} + \varepsilon_{ait}, \tag{4}$$

where a indicates age category with $a \in \{< 5, 5\text{–}64, > 64\}$, i denotes the second administrative level (ADM2),[11] s refers to the first administrative level (ADM1), c denotes country, and t indicates years. Thus, M_{ait} is the age-specific all-cause mortality rate in ADM2 unit i in year t. α_{ai} is a vector of fixed effects for $age \times ADM2$, and δ_{act} is a vector of fixed effects that allow for shocks to mortality that vary at the $age \times country \times year$ level.

Before describing the functional form for $g_a(\cdot)$, we note that the temperature data are provided at the grid-cell-by-day level. As detailed in Online Appendix B.2.4, we align gridded daily temperatures with annual administrative mortality records using a method that allows for the recovery of a nonlinear relationship between mortality and temperature that occurs at the grid cell level, even though equation (4) is estimated at a higher level of aggregation (Hsiang 2016). The nonlinear transformations of daily temperature are captured by the annual, ADM2-level vector $\boldsymbol{T}_{it}$.

In our main specification, $\boldsymbol{T}_{it}$ is represented by fourth-order polynomials of daily average temperatures, summed across the year. This model strikes a balance between providing sufficient flexibility to capture important nonlinearities, parsimony, and limiting demands on the data. In a set of robustness checks, we explore the sensitivity of the results to alternative functional forms for temperature, such as binned daily average temperatures, restricted cubic splines, and a two-part linear spline. Analogous to temperature, we summarize daily grid-level precipitation in the annual ADM2-level vector $\boldsymbol{R}_{it}$. We construct $\boldsymbol{R}_{it}$ as a second-order polynomial of daily precipitation, summed

11. This is usually the case. However, as shown in Table I, the EU data are reported at Nomenclature of Territorial Units for Statistics second (NUTS2) level, and Japan reports mortality at the first administrative level.

across the year, and estimate an age- and country-specific linear function of this vector, represented by $q_{ac}(\cdot)$.

The effect of weather realizations $\boldsymbol{T}_{it}$ on mortality is identified from the plausibly random year-to-year variation in temperature in a geographic unit. Specifically, the $age \times ADM2$ fixed effects α_{ai} ensure that we isolate within-location year-to-year variation in temperature and rainfall exposure, which is as good as randomly assigned. The $age \times country \times year$ fixed effects δ_{act} account for any time-varying trends or shocks to age-specific mortality rates that are unrelated to the climate, although we also explore robustness to alternative sets of fixed effects.

The mortality-temperature response function $g_a(\cdot)$ depends on *TMEAN*, the sample period average annual temperature, and the log of *GDPpc*, the sample period average of annual GDP per capita. The model does not include uninteracted terms for *TMEAN* and *GDPpc* because they are collinear with α_{ai}, which shuts down the possibility of the climate influencing the mortality rate equally on all days, regardless of daily temperature. We impose this assumption because we define climate adaptation to be actions or investments that reduce the risk from temperatures that threaten human well-being, as is common in the literature (e.g., Hsiang 2016). Our analysis therefore allows the benefits (and, as discussed later, the costs) of adaptation to influence the shape of the mortality-temperature relationship, but not its level.

In practice, we interact *TMEAN* and $\log(GDPpc)$ with each of the elements of the temperature vector $\boldsymbol{T}_{it}$, which, as we noted, is a fourth-order polynomial in our preferred specification. We estimate equation (4) without any regression weights because we are explicitly modeling heterogeneity in treatment effects rather than integrating over it, and because we find that population weights generally lead to less precise estimates, as is common with data that represent group-level averages (Solon, Haider, and Wooldridge 2015). More details on the implementation of this regression are in Online Appendix D.1.

A central challenge in understanding the extent of adaptation is that there exists no experimental or quasi-experimental variation in climate as opposed to weather. Put simply, meaningful variation in climate in a location is not available in recorded history. So, while plausibly random year-to-year fluctuations in temperature within locations are used to identify the effect of weather events in equation (4), we must use cross-sectional variation in climate, as well as in income, between locations to

estimate heterogeneity in the mortality-temperature relationship. We therefore interpret our heterogeneity results as associational.

Nevertheless, we believe this model's estimates are informative about the effect of climate change on mortality for several reasons, including: adding alternative sources of heterogeneity in mortality sensitivity to temperature has little effect on the estimated response functions; the model performs well out of sample on a variety of cross-validation tests; and estimated response functions are robust to a host of alternative specifications. These tests are discussed in detail in Sections IV.C and V.B.

IV.B. Empirical Results

Before presenting results from the estimation of equation (4), we show results using a model without interactions, yielding average effects of temperature on mortality across individuals in each age group. This model is detailed in Online Appendix D.2, but uses the same set of fixed effects and controls as equation (4). Online Appendix Figure D.3 displays the resulting average mortality-temperature responses for each age group. Consistent with prior literature (e.g., Deschênes and Moretti 2009; Heutel, Miller, and Molitor 2017), we uncover substantial heterogeneity across age groups in our multicountry sample. On average, we find that people over the age of 64 experience approximately 4.7 extra deaths per 100,000 for a day at 35°C (95°F) compared to a day at 20°C (68°F), a substantially larger effect than that for younger cohorts, which exhibit little response. This age group is also more severely affected by cold days; estimates suggest that people over the age of 64 experience 3.4 deaths per 100,000 for a day at −5°C (23°F) compared to a day at 20°C, while there is a small and statistically insignificant mortality response to these cold days for other age categories. Overall, these results demonstrate that the elderly are disproportionately harmed by additional hot days and disproportionately benefit from reductions in cold days.

Tabular results for the estimation of equation (4), which models heterogeneity in the mortality-temperature response across our sample, are reported in Online Appendix Table D.1 for each age group. Because these terms are difficult to interpret, we present the results visually by dividing the sample into nine subsamples, based on terciles of climate and income. We then plot predicted response functions at the mean value of climate and income in the nine subsamples, using the coefficients from estimation of

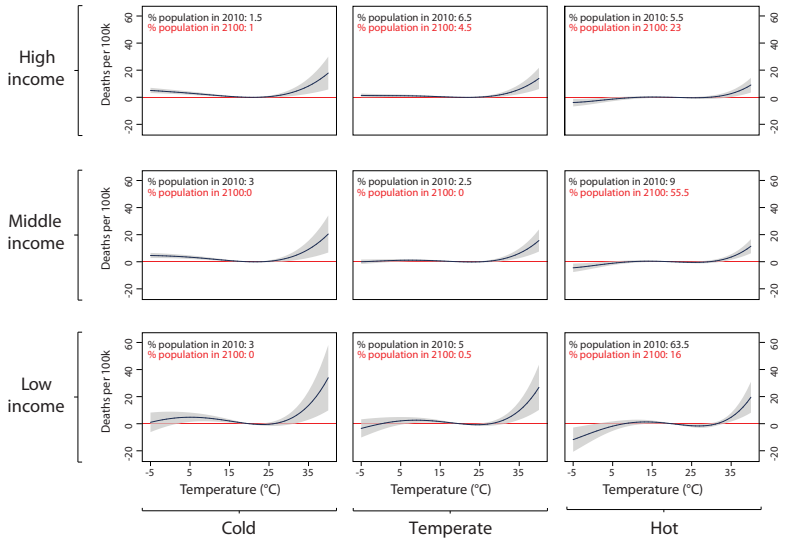

FIGURE I

Heterogeneity in the Mortality-Temperature Relationship (Age > 64 Mortality Rate)

Each panel represents a predicted mortality-temperature response function for the > 64 age group for a subset of the income-average temperature covariate space in the data sample. Response functions in the lower left apply to the low-income, cold regions of the sample, and those in the upper right apply to the high-income, hot regions of the sample. Regression estimates are from a fourth-order polynomial in daily average temperature and are estimated using GMFD weather data with a sample that was winsorized at the 1% level on the top end of the distribution only. All response functions are estimated jointly in a stacked regression model that is fully saturated with age-specific fixed effects, and where each temperature variable is interacted with each covariate. Values in the top left corner of each panel show the percentage of the global population that reside in each in-sample tercile of average income and average temperature in 2010 (top row) and as projected in 2100 (bottom row, SSP3). Other age groups are shown in Online Appendix Figures D.1 and D.2.

equation (4). The result is a set of predicted mortality-temperature response functions that vary across the joint distribution of income and average temperature in the sample data. The resulting response functions are shown in Figure I for the > 64 age category (other age groups are shown in Online Appendix D.1), where average incomes are increasing across subsamples vertically and average temperatures are increasing across subsamples horizontally.

The Figure I results are broadly consistent with the economic prediction that people adapt to their climate and that income is protective. For example, in each income tercile in Figure I, the effect of hot days (days $> 35^{\circ}$C) on mortality rates declines as one moves from left (cold climates) to right (hot climates). Presumably, this reflects individuals' and societies' compensatory adaptations in response to their climate (e.g., greater penetration of air conditioning in hot climates than in cold ones). With respect to income, Figure I reveals that moving from the bottom (low income) to top (high income) in a climate tercile causes a substantial flattening of the response function, especially at high temperatures. Two statistics help summarize the findings in Figure I. First, moving from the coldest to the hottest tercile saves on average 7.9 (p-value $= .06$) deaths per 100,000 at 35°C. Second, moving from the poorest to the richest tercile saves approximately 5.0 (p-value $= .1$) deaths per 100,000 at 35°C for the > 64 age category.[12]

As shown in Online Appendix D.1, qualitatively similar results are recovered for other age groups. This is consistent with conventional wisdom that protection from extreme temperatures is a normal good, although the effect of income on the mortality-temperature relationship would not be judged statistically significant by conventional criteria for the > 64 age category (see Online Appendix Table D.1).

IV.C. Sensitivity Analyses

In Online Appendix D, we present additional empirical results and a variety of sensitivity analyses that probe the robustness of the results presented in the previous subsection. For example, Online Appendix Table D.2 reports on the robustness of the estimated mortality-temperature relationship to alternative specifications, including different spatial and temporal controls. Online Appendix Figure D.4 shows that mortality-temperature responses are similar across alternative functional-form

12. These values are calculated by predicting the mortality-temperature relationship at the mean value of climate and income in each tercile of the estimating sample, using coefficients from the estimation of equation (4). For example, we evaluate $\hat{g}_a(\cdot)$ at the average climate and income observed in the poorest $\frac{1}{3}$ of administrative units (poorest tercile) or the hottest $\frac{1}{3}$ of administrative units (hottest tercile). We then difference the mortality response to 35°C between two terciles (e.g., coldest minus hottest). p-values are computed using a standard t-test on the linear combination of coefficients.

assumptions for temperature, as well as across alternative climate data sets. Online Appendices D.4 and D.5 show that predicted mortality-temperature relationships are qualitatively unchanged when we use alternative characterizations of the climate or if we omit precipitation controls, respectively. Finally, Online Appendix D.6 shows that adding other candidate determinants of heterogeneity in the mortality-temperature relationship to equation (4), such as institutional quality, doctors per capita, and educational attainment, generates very similar predicted response functions, supporting our assumption that climate and income are key determinants of the shape of the response function.

V. Projections of Climate Change Effects on Future Mortality Rates

This section begins by providing practical expressions for the three measures of the mortality effects of climate change defined in Section II. Section V.B then details the methods employed to extrapolate mortality-temperature relationships to the parts of the world where historical mortality data are unavailable and to future time periods. Finally, Section V.C reports on the projected mortality effects of climate change, accounting for climate model and econometric uncertainty. The article's ultimate aim is to develop an estimate of the full mortality risk of climate change (i.e., the sum of the increase in deaths and adaptation costs shown in equation (3)), but adaptation costs are not observed directly. In Section VI, we use a stylized revealed-preference approach to infer adaptation costs, which allows for a complete measure.

V.A. Practical Expressions for Three Measures of the Mortality Effects of Climate Change

Here we translate the three measures of the mortality effects of climate change defined in Section II (equations (2), (2a), and (2b)) into expressions that can be directly computed from the empirical results shown in Section IV. The empirical estimation of each of these measures is reported below in units of deaths per 100,000, although it is straightforward to monetize these measures using estimates of the VSL, and we do so in the next section. Here and throughout this subsection, subscripts for impact regions and age groups are omitted for clarity, although all measures of the mortality effects of climate change are computed separately for each age group, impact region, and year.

First, the mortality effects of climate change, as defined in equation (2), are empirically computed as:

$$\begin{aligned} &\textit{mortality effects of climate change} \\ &= \hat{g}(\boldsymbol{T}_t, TMEAN_t, \log(GDPpc)_t) \\ &- \hat{g}(\boldsymbol{T}_{t_0}, TMEAN_{t_0}, \log(GDPpc)_t), \end{aligned} \tag{2′}$$

where $\hat{g}(\cdot)$ represents the fitted values from estimation of equation (4). This expression accounts for endogenous responses to both the changing climate and evolving incomes. Note that in equation (2′), the second term represents a counterfactual predicted mortality rate that would be realized under current temperatures, but in a population that benefits from rising incomes. This counterfactual is used to isolate the role of climate change from the benefits of income growth in determining mortality's sensitivity to temperature.

Second, the mortality effects of climate change without income growth or adaptation, defined in equation (2a), is a benchmark expression often employed in previous work that assumes that mortality sensitivity to temperature does not change in response to future incomes or temperatures. It is empirically estimated as:

$$\begin{aligned} &\textit{mortality effects of climate change (without income} \\ &\textit{growth or adaptation)} = \hat{g}(\boldsymbol{T}_t, TMEAN_{t_0}, \log(GDPpc)_{t_0}) \\ &- \hat{g}(\boldsymbol{T}_{t_0}, TMEAN_{t_0}, \log(GDPpc)_{t_0}). \end{aligned} \tag{2a′}$$

Finally, the mortality effects of climate change without adaptation, defined in equation (2b′), captures the change in mortality rates that would be expected if populations became richer, but they did not respond optimally to warming. It is calculated as:

$$\begin{aligned} &\textit{mortality effects of climate change (without adaptation)} \\ &= \hat{g}(\boldsymbol{T}_t, TMEAN_{t_0}, \log(GDPpc)_t) \\ &- \hat{g}(\boldsymbol{T}_{t_0}, TMEAN_{t_0}, \log(GDPpc)_t). \end{aligned} \tag{2b′}$$

When computing equations (2′), (2a′), and (2b′), we define the baseline period t_0 to be the years 2001–2010, so we are measuring

the effect of climate change since this period.[13] These three measures are all reported below using the estimates of $\hat{g}(\cdot)$ shown in Section IV in combination with projections of income and climate from data sets described in Section III.

V.B. *Methods for Projecting the Mortality Effects of Climate Change*

1. *Spatial Extrapolation.* The fact that carbon emissions are a global pollutant requires that estimates of climate damages used to inform an SCC must be global in scope. A key challenge for generating such globally comprehensive estimates in the case of mortality is the absence of data throughout many parts of the world. Often, registration of births and deaths does not occur systematically. Although we have, to the best of our knowledge, compiled the most comprehensive mortality data file ever collected, the 40 covered countries only account for 38% of the global population (55% if India is included, although it only contains all-age mortality rates). This leaves more than 4.2 billion people unrepresented in the sample of available data, which is especially troubling because these populations have incomes and live in climates that may differ from the parts of the world where data are available.

To achieve the global coverage essential to understanding the costs of climate change, we use the results from the estimation of equation (4) on the observed 38% global sample to estimate the sensitivity of mortality to temperature everywhere, including the unobserved 62% of the world's population. Specifically, the results from this model enable us to use two observable characteristics, average temperature and income, to predict the mortality-temperature response function for each of our 24,378 impact regions.

To see how this is done, we note that the projected response function for any impact region r requires three ingredients. The first are the estimated coefficients $\hat{g}_a(\cdot)$ from equation (4). The second are estimates of GDP per capita at the impact region level. Third is the long-run average annual temperature for each impact region.

Using these data, we predict the shape of the response function for each age group a, impact region r, and year t, up to

13. While anthropogenic warming has been detected in the climate record far earlier than 2001–2010, we estimate effects of climate change only since this period.

a constant: $\hat{g}_{art} = \hat{g}_a(\boldsymbol{T}_{rt}, TMEAN_{rt}, \log(GDPpc)_{rt})$. The various fixed effects in equation (4) are unknown and omitted, since they were nuisance parameters in the original regression.

This results in a unique, spatially heterogeneous, and globally comprehensive set of predicted response functions for each location on Earth.

The accuracy of the predicted response functions will depend partly on the ability of estimated equation (4) to capture responses in regions where mortality data are unavailable. An imperfect but helpful exercise when considering whether our model is representative is to evaluate the extent of common overlap between the two samples. Figure II, Panel A shows this overlap in 2015, where the gray squares reflect the joint distribution of GDP and climate in the full global partition of 24,378 impact regions and the overlaid squares represent the distribution only for the impact regions in the sample used to estimate equation (4). It is evident that temperatures in the global sample are generally well covered by our data, although we lack coverage for the poorer end of the global income distribution because of the absence of mortality data in poorer countries.

To assess the performance of our model in predicting mortality-temperature relationships out-of-sample, Online Appendices D.7 and D.8 report on multiple custom cross-validation exercises designed to mimic the article's spatial extrapolation. The model in equation (4) performs well in all out-of-sample tests, both when compared to measures of in-sample model fit and when compared to the out-of-sample performance of models that omit all or some of the interaction effects, as is done in much of the prior literature (e.g., Deschênes and Greenstone 2011; Hsiang et al. 2017). However, this model generates conservative predictions of mortality effects of climate change in India, a hot and poor region that is not used in estimation due to its lack of age-specific mortality rates.

2. *Temporal Extrapolation.* As detailed in equation (2′), we allow each impact region's mortality-temperature response function to evolve over time, reflecting projected changes in climate and income that come from a set of internationally standardized and widely used scenarios. Specifically, we model the evolution of response functions in region r and year t based on these projections and the estimation results from fitting equation (4).

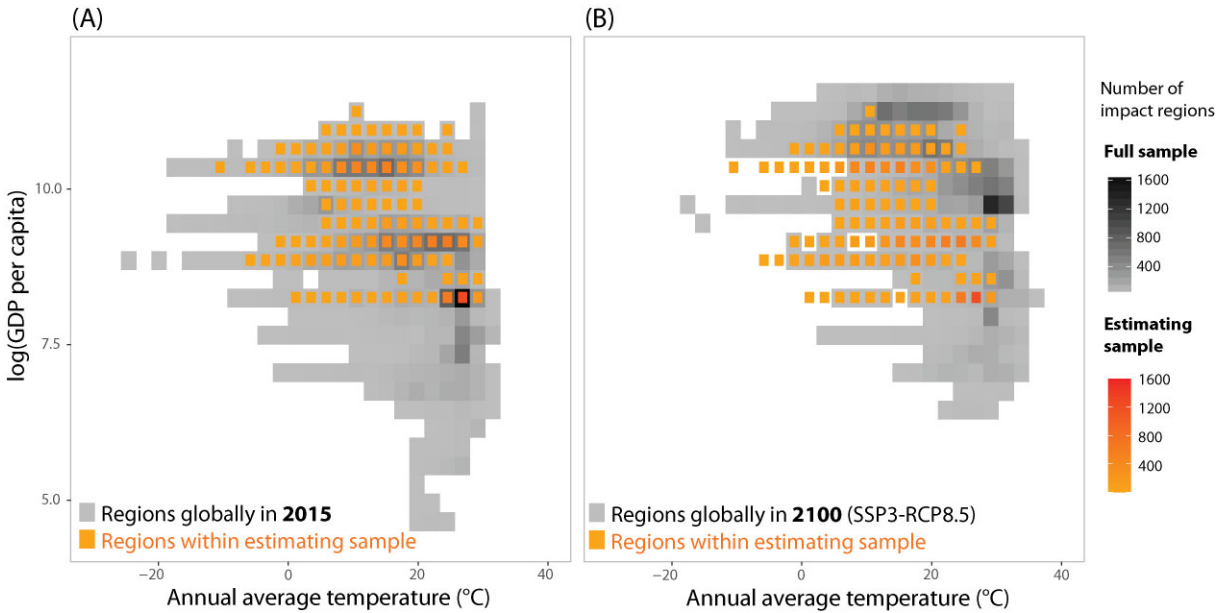

FIGURE II

Joint Coverage of Income and Long-Run Average Temperature for Estimating and Full Samples

Panels show the joint distribution of income and long-run average annual temperature in the estimating sample as compared to the global sample of impact regions. Panel A shows in gray-black the global sample for impact regions in 2015. Panel B shows in gray-black the global sample for impact regions in 2100 under a high-emissions scenario (RCP8.5) using climate model CCSM4 and a median-growth scenario (SSP3). In both panels, the estimating sample indicates coverage for impact regions in the estimating sample using 2015 values of income and long-run average annual temperature.

Some details about these projections are worth noting. First, a 13-year moving average of income per capita in region r is calculated using national forecasts from the SSP, combined with a within-country allocation of income based on present-day nighttime lights (see Online Appendix B.3.2), to generate a new value of $\log(GDPpc)_{rt}$.

The length of this time window is chosen based on a goodness-of-fit test across alternative window lengths (see Online Appendix E.1). Second, a 30-year moving average of temperatures for region r is updated in each year t to generate a new level of $TMEAN_{rt}$. The response curves $\hat{g}_{art} = \hat{g}_a(\boldsymbol{T}_{rt}, TMEAN_{rt}, \log(GDPpc)_{rt})$ are calculated for each impact region for each age group in each year with these updated values of $TMEAN_{rt}$ and $\log(GDPpc)_{rt}$.

Third, Figure II, Panel B shows that over the coming decades, temperatures and incomes are predicted to rise beyond the support of the global cross section in our historical data. Thus, we impose two constraints on our projections, guided by economic theory and by the physiological literature, to ensure that future response functions are consistent with the fundamental characteristics of mortality-temperature responses in the historical record. The first assumption ensures that the response function is weakly monotonic around an empirically estimated, location-specific, optimal mortality temperature, called the minimum mortality temperature (MMT). The second assumption is that rising income cannot make individuals worse off, in the sense of increasing the temperature sensitivity of mortality. These assumptions and their implementation are detailed in Online Appendix E.2.

With these two constraints, we project annual effects of climate change separately for each impact region and age group from 2001 to 2100.[14] Specifically, we apply projected changes in the climate to each region's response function, which is evolving as climate and income evolve. The nonlinear transformations of daily average temperature that are used in the function $g_a(\cdot)$ are computed under the RCP4.5 and RCP8.5 emissions scenarios for all 33 climate projections in the SMME (as described in Section III.B). This distribution of climate models captures uncertainties in the climate system through 2100.

14. When computing the mortality partial SCC, we include mortality effects of climate change after 2100. See Section VII.B for details on our approach to extrapolating beyond years for which standard climate and socioeconomic projections are available.

To assess the performance of our model in predicting mortality-temperature relationships in new time periods, Online Appendix D.7 reports on a cross-validation exercise that subsamples data based on time, showing that overall performance is high when compared with a benchmark model. However, we do find that equation (4) occasionally overestimates or underestimates future mortality sensitivity to hot days in some age groups and for some income levels (see Online Appendix Figure D.10). To address this concern, Online Appendix F.4 explores the sensitivity of our main climate change projections to alternative assumptions about the rates of adaptation.

3. *Uncertainty.* An important feature of the analysis is to characterize the uncertainty inherent in these projections of the mortality effects of climate change.[15] As discussed already, we construct estimates of the mortality effects of climate change for each of 33 distinct climate projections in the SMME that together capture the uncertainty in the climate system.[16] In addition, uncertainty in the estimates of $\hat{g}_a(\cdot)$ is an important second source of uncertainty in our projected effects that is independent of physical uncertainty.

To account for both of these sources of uncertainty, we execute a Monte Carlo simulation. First, for each age category, we randomly draw a set of parameters corresponding to the terms composing $\hat{g}_a(\cdot)$ from an empirical multivariate normal distribution characterized by the covariance between all of the parameters from the estimation of equation (4).[17] Second, using these parameters in combination with location- and time-specific values of income and average climate provided by a given SSP scenario and RCP-specific climate projection from the 33 climate projections in

15. See Burke et al. (2015) for a discussion of combining physical and econometric uncertainty in studies of climate change effects.

16. Note that while the SMME fully represents the tails of the climate sensitivity distribution as defined by a probabilistic simple climate model (see Online Appendix B.2.3), there remain important sources of climate uncertainty that are not captured in our projections, due to the limitations of both the simple climate model and the GCMs. These include some climate feedbacks that may amplify the increase of GMST, as well as some factors affecting local climate that are poorly simulated by GCMs.

17. Note that coefficients for all age groups are estimated jointly in equation (4), such that across-age-group covariances are accounted for in this multivariate distribution.

the SMME, we construct a predicted response function for each of our 24,378 impact regions. Third, with these response functions in hand, we use daily weather realizations from the corresponding simulation to calculate the mortality effects of climate change (equations (2′), (2a′), and (2b′)) for each impact region for each year between 2001 and 2100. Finally, this process is repeated until approximately 1,000 projection estimates are complete for each impact region, age group, and RCP-SSP combination.

The resulting calculation is computationally intensive, requiring ∼94,000 hours of CPU time across all scenarios. When reporting projected effects in any given year, we show summary statistics (e.g., mean, median) for reasons of parsimony, although this entire distribution is available. In Section VII, we value the uncertainty characterized by this distribution following Nath et al. (2022) in undertaking "certainty equivalence" calculations with standard risk aversion parameters.

V.C. Results: the Mortality Effects of Climate Change

1. *Spatial Extrapolation of Temperature Sensitivity.* Figure III, Panel A reports predicted mortality-temperature response functions for the > 64 age category for the impact regions that fall within the countries in our mortality data set (labeled "in-sample").[18] These predicted responses are plotted for each impact region using 2015 values of income and climate. Despite a shared overall shape, this figure reveals substantial heterogeneity across regions in this temperature response. Geographic heterogeneity in the sample is shown for hot days in the map in Panel B, where shading indicates the marginal effect of a day at 35°C, relative to a day at a location-specific minimum mortality temperature. Just as in Figure I, the predicted mortality response to very hot days is greatest in places with cool climates and in those with low incomes.

Figure III, Panels C and D show analogous plots, again using 2015 data on location-specific average income and climate, but here filling in the estimated mortality response to a hot day in locations without mortality data (labeled "global"). The predicted responses imply that a 35°C day increases the global average mortality rate for the oldest age category by 10.1 deaths per 100,000 relative to a location-specific minimum mortality temperature,

18. Online Appendix Figure D.5 shows analogous results for other age groups.

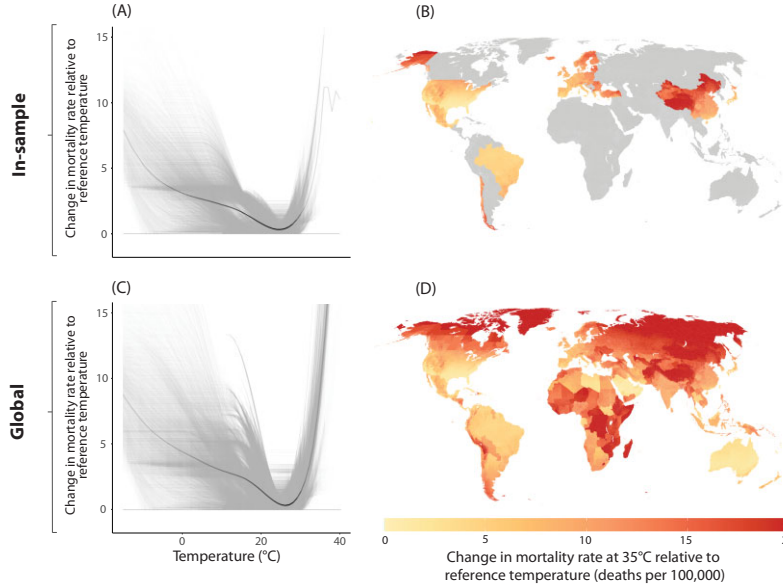

FIGURE III

Using Income and Climate to Predict Current Response Functions Globally (Age > 64 Mortality Rate)

In Panels A and C, gray lines are predicted response functions for impact regions, each representing a population of 276,000 on average. Solid black lines are the unweighted average of the gray lines, where the opacity indicates the density of realized temperatures (Hsiang 2013). Panels B and D show each impact region's mortality sensitivity to a day at 35°C, relative to a location-specific minimum mortality temperature. The top row shows all impact regions in the estimating sample, and the bottom row shows extrapolation to all impact regions globally. Predictions shown are for 2015 using the SSP3 socioeconomic scenario and climate model CCSM4 under the RCP8.5 emissions scenario. Online Appendix Figure D.5 shows analogous results for other age groups.

although there is substantial heterogeneity across the planet. The effect in locations without mortality data is 11.7 deaths per 100,000, versus 7.8 in the sample of countries for which mortality data are available, largely driven by the fact that the sample with mortality data represents wealthier locations where temperature responses are more muted.

2. *Projection of the Mortality Effects of Climate Change.* The previous subsection demonstrated that the model of heterogeneity outlined in equation (4) allows us to extrapolate mortality-temperature relationships to regions of the world with-

out mortality data today. This subsection uses those results, in combination with downscaled projections of income and climate, to estimate the mortality effects of climate change at global scale and over time, following the methods in Section V.B. Here, we show results relying on income and population projections from the socioeconomic scenario SSP3 because its historic global growth rates in GDP per capita and population match observed global growth rates over the 2000–2018 period much more closely than other SSPs (see Online Appendix Table B.3). Online Appendix F shows results using SSP2 and SSP4, and the article's approach can be applied to any available socioeconomic scenario.

Figure IV shows the spatial distribution of the mortality effects of climate change (equation (2′)) in 2100 under the emissions scenario RCP8.5. Other measures of climate change effects (equations (2a′), (2b′), and (3′)) are mapped in Online Appendix Figure F.1. To construct these estimates, we calculate equation (2′) for each impact region in 2100, separately for each age group. The map displays the spatial distribution of the mean estimate across our ensemble of Monte Carlo simulations, accounting for both climate and statistical uncertainty and pooling across all age groups.[19] The density plots for select cities show the full distribution of effects across all Monte Carlo simulations, with the white line equal to the mean estimate displayed on the map.

Figure IV makes clear that the mortality effects of climate change are distributed unevenly around the world, even when accounting for the benefits of income growth and adaptation. Despite the gains from adaptation shown in Online Appendix Figure E.2, there are large increases in mortality rates in the global South. For example, in Accra, Ghana, climate change is predicted to lead to approximately 100 more days above 32°C (~90°F) a year and cause 140 additional deaths per 100,000 annually under RCP8.5 in 2100. This is a large effect, roughly equal to a 17% increase in Accra's current overall mortality rate. If adaptation to climate and benefits of income growth were ignored (as in equation (2a′)), climate change would be predicted to cause 260 additional deaths per 100,000 in Accra in this scenario. In con-

19. When calculating mean values across estimates generated for the 33 climate models that form our ensemble, we use model-specific weights. These weights are constructed as described in Online Appendix B.2.3 to accurately reflect the full probability distribution of temperature responses to changes in greenhouse gas concentrations.

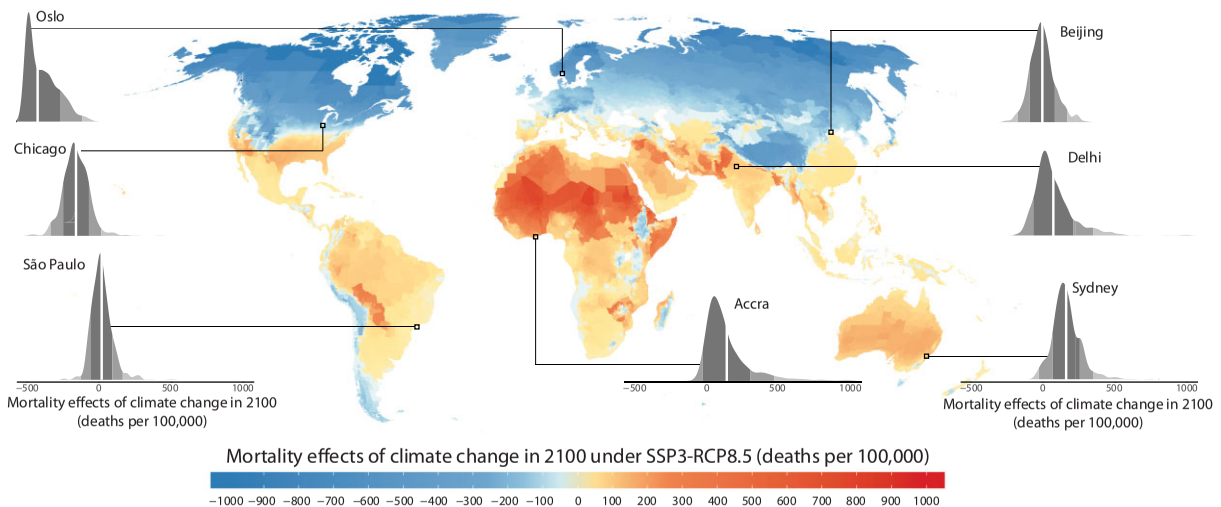

FIGURE IV

The Mortality Effects of Future Climate Change

The map indicates estimates of the mortality effects of climate change (equation (2′)), measured in units of deaths per 100,000 population, in 2100. Estimates come from a model accounting for the benefits of adaptation and income growth, and the map shows the climate model weighted mean estimate across Monte Carlo simulations conducted on 33 climate models; density plots for select regions indicate the full distribution of estimated effects across all Monte Carlo simulations. In each density plot, solid white lines indicate the mean estimate shown on the map, while shading indicates 1, 2, or 3 standard deviations from the mean. All values shown refer to the RCP8.5 emissions scenario and the SSP3 socioeconomic scenario. See Online Appendix Figure F.6 for an analogous map of effects for RCP4.5 and SSP3.

trast, there are gains in many impact regions in the global North, including Berlin, Germany, where climate change is predicted to save approximately 150 lives per 100,000 annually when climate adaptation and benefits of income growth are accounted for. These avoided deaths occur because of a substantial reduction in the number of deadly cold days and amount to a 15% decline in Berlin's current mortality rate.

Figure V plots predictions of the global average mortality effects of climate change following equations (2′), (2a′), and (2b′) under emissions scenario RCP8.5. These three measures of mortality effects are calculated for the 24,378 impact regions and then aggregated to the global level. In Panel A, each line shows a mean estimate for the corresponding measure and year. Averages are taken across the full set of Monte Carlo simulation results from all 33 climate models, and all draws from the empirical distribution of estimated regression parameters, as described above. In Panel B, the 25th–75th and 10th–90th percentile ranges of the Monte Carlo simulation distribution are shown for the mortality effects of climate change (equation (2′)); the solid green line represents the same average value in both panels. Boxplots to the right summarize the distribution of mortality effects for both RCP8.5 and the moderate-emissions scenario RCP4.5; Online Appendix Figure F.7 replicates the entire figure for RCP4.5.

Figure V, Panel A illustrates that the global mortality effects of climate change would be 221 deaths per 100,000 by 2100, on average across simulation runs, if the beneficial effects of adaptation and income were shut down. This is a large estimate; it is roughly equivalent in magnitude to all global deaths from cardiovascular disease today (WHO 2018).

However, our estimates suggest that future income growth and adaptation to climate will substantially reduce these effects. Higher incomes lower the predicted mortality effects of climate change to an average of 104 deaths per 100,000 in 2100, although this estimate exhibits substantial uncertainty (see Online Appendix Table D.1 and Online Appendix Figure F.3). Climate adaptation reduces this further to 73 deaths per 100,000 (solid line). Although much lower than the projection assuming no adaptation or income growth, these estimates remain economically meaningful—they are about six times larger than the current fatality rate from automobile accidents in the United States (12 per 100,000) and amount to 60% of the 2020 reported U.S. fatality rate from COVID-19 (116 per 100,000).

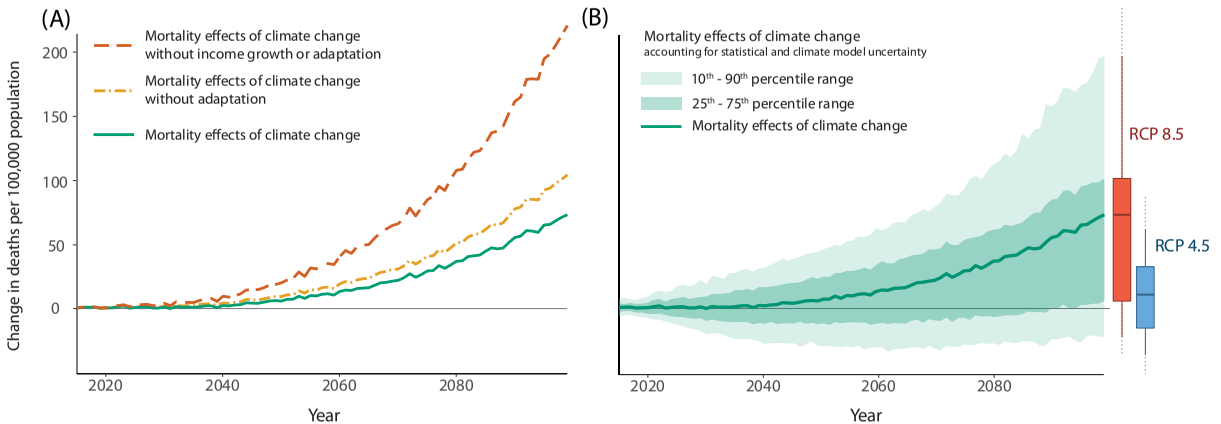

FIGURE V

Time Series of Projected Mortality Effects of Climate Change

All lines show projected mortality effects of climate change across all age categories and are represented by a mean estimate across a set of Monte Carlo simulations accounting for climate model and statistical uncertainty. In Panel A, each line represents one of three measures of the mortality effects of climate change. Dashed (equation (2a′)): mortality effects of climate change without income growth or adaptation. Dashed-dotted: (equation (2b′)): mortality effects of climate change without adaptation. Solid (equation (2′)): mortality effects of climate change. Panel B shows the 10th–90th percentile range of the Monte Carlo simulations for the mortality effects of climate change (equivalent to the solid line in Panel A), as well as the mean and interquartile range. The boxplots show the distribution of mortality effects of climate change in 2100 under both RCPs. All line estimates shown refer to the RCP8.5 emissions scenario and all line and boxplot estimates refer to the SSP3 socioeconomic scenario. Online Appendix Figure F.7 shows the equivalent for SSP3 and RCP4.5.

The large predicted benefits of income growth and climate adaptation are driven by substantial changes in the mortality-temperature relationship over the twenty-first century. For example, for the > 64 age group, the average global increase in the mortality rate on a 35°C day (relative to a day at location-specific minimum mortality temperatures) declines by roughly 75% between 2015 and 2100, going from 10.1 per 100,000 to just 2.4 per 100,000 in 2100 (see Online Appendix Figure E.2) under socioeconomic scenario SSP3. Increasing incomes account for 77% of the decline, with adaptation to climate explaining the remainder; income gains account for 89% and 82% of the decline for the < 5 and 5–64 categories, respectively.

The values in Figure V, Panel A are mean values aggregated across all Monte Carlo simulation runs, but the full distribution of the estimated mortality effects of climate change is right-skewed (Panel B). Indeed, there is meaningful mass in the right tail. As evidence of this, the median value of the mortality effects of climate change under RCP8.5 at the end of the century is 42 deaths per 100,000, as compared to the mean value of 73, and the 10th to 90th percentile range is [−22, 197].

Figure V, Panel B and Online Appendix Figure F.5 can be used to develop estimates of the expected benefits of emissions mitigation. The mean estimate of the mortality effects of climate change falls from 73 deaths per 100,000 under RCP8.5 to 11 deaths per 100,000 under the emissions stabilization scenario of RCP4.5. For RCP4.5, the median end-of-century estimate is 4, and the 10th–90th percentile range is [−36, 62].

As a point of comparison to the limited literature estimating the global mortality consequences of climate change, we contrast these results to the FUND model, which is unique among the IAMs for calculating separate mortality effects as a component of its SCC calculation. It is difficult to make a direct comparison due to differences in socioeconomic and emissions scenarios, different treatments of adaptation, and the inclusion of diarrhea and vector-borne diseases in FUND. Furthermore, the FUND model was calibrated decades ago based on limited mortality data from just 20 cities, largely in wealthy and temperate locations. Nevertheless, the closest analog is to compare our mean estimate of the global mortality effects of climate change, a change of 73 deaths per 100,000 by 2100 under RCP8.5, to FUND's reference scenario change of 0.33 deaths per 100,000 in the same year

(Anthoff and Tol 2014).[20] It is apparent that this study's use of modern econometric tools and large-scale data sets leads to much larger estimates of climate change's effect on human mortality.

Before proceeding, we note that in some instances it is necessary to extrapolate response functions to temperatures outside of those historically observed, based on the fourth-order polynomial in daily temperature estimated in equation (4). To explore the possibility that out-of-sample behavior is disproportionately influencing our results, Online Appendix F.3 reports on two sensitivity tests that impose additional restrictions on the mortality-temperature relationship for out-of-sample temperatures. These restrictions are (i) that the mortality-temperature response function is flat for all temperatures outside the observed range; and (ii) that the mortality-temperature response function increases linearly for all temperature outside the observed range. These additional restrictions have negligible effects on our estimated mortality effects of climate change, suggesting that out-of-sample behavior is not driving the results.

VI. The Full Mortality Risk of Climate Change

The last section found meaningful estimated benefits from climate-induced adaptation. This section develops a revealed-preference approach to estimate the costs of these adaptations. Specifically, we use observed differences in the sensitivity of mortality to temperature to infer measures of location-specific adaptation costs. We assume that differential mortality sensitivities to temperature are due to differential uptake of costly adaptive technologies, behaviors, or other investments. Indeed, if these investments were costless, we would expect universal uptake, such that mortality rates would exhibit little to no response to temperature across the globe. The approach therefore assumes that differences in the mortality

20. This value was calculated by running the MimiFUND model (v3.12.1) and extracting global additional deaths from all modeled causes. Additional deaths are calculated as the difference between the reference scenario in MimiFUND and a baseline in which temperature and CO_2 are held constant at their 2005 levels. See Online Appendix Table B.4 for details on the differences between our approach, that of FUND, and that of other empirical estimates of the effects of climate change on mortality.

sensitivity to temperature between locations can be the basis for inferring adaptation costs. This revealed-preference approach relies on a strong set of simplifying assumptions, but it can be directly estimated with available data, even though the many dimensions of adaptation and their costs are generally unobservable.

After outlining our approach for recovering adaptation costs, this section presents projections of the full mortality risk of climate change into the future, accounting for the benefits and costs of adaptation following equation (3). We also demonstrate how the effects of climate change on mortality and on mortality-related adaptation costs are projected to occur unequally around the world.

VI.A. Revealed-Preference Approach to Infer Adaptation Costs

This subsection sketches an outline of the revealed-preference approach to recovering adaptation costs.[21] Online Appendix A provides a more detailed description.

Consider a single representative agent who derives utility in each time period t from consumption of a numeraire good x_t. This agent faces mortality risk $f_t = f(\boldsymbol{b}_t, \boldsymbol{c}_t)$, which depends on the weather and on adaptive behaviors and investments captured by the composite good $\boldsymbol{b}_t$. As discussed in Section II, changes in the climate $\boldsymbol{C}_t$ influence mortality risk through altering weather realizations $\boldsymbol{c}_t$ and through changing beliefs about the weather, hence changing adaptive behaviors $\boldsymbol{b}_t$.[22]

In bringing this framework to our empirical analysis, we allow for 24,378 representative agents, one for each of the impact regions. Each region's representative agent chooses consumption of the numeraire x_t and of the composite good $\boldsymbol{b}_t$ in each period to maximize utility given her expectations of the weather, subject to an exogenous budget constraint and conditional on the climate. We let $\tilde{f}(\boldsymbol{b}_t, \boldsymbol{C}_t) = \mathbb{E}_{\boldsymbol{c}_t}[f(\boldsymbol{b}_t, \boldsymbol{c}(\boldsymbol{C}_t)) \mid \boldsymbol{C}_t]$ represent the expected

21. This approach is related to Schlenker, Roberts, and Lobell (2013), who show that estimates of differences in the sensitivity of maize yields to temperature across locations can be used to infer the costs of adapting to warming.

22. Recall that we define the climate $\boldsymbol{C}_t$ as the joint probability distribution over a vector of weather conditions that can be expected to occur in period t. The random vector of weather realizations drawn from this distribution is denoted as $\boldsymbol{c}(\boldsymbol{C}_t)$.

probability of death. This agent therefore solves:

$$\max_{\boldsymbol{b}_t, x_t} \; u(x_t)[1 - \tilde{f}(\boldsymbol{b}_t, \boldsymbol{C}_t)] \;\; s.t. \;\; Y_t \geqslant x_t + A(\boldsymbol{b}_t), \tag{5}$$

where $A(\boldsymbol{b}_t)$ represents expenditures for all adaptive investments, and Y is income that is assumed to be exogenous. Under these assumptions, the first-order conditions of equation (5) define optimal adaptation as a function of income and the climate: $\boldsymbol{b}^*(Y_t, \boldsymbol{C}_t)$, which we sometimes denote as $\boldsymbol{b}_t^*$ for simplicity.

We use this framework to derive an empirically tractable expression for the full mortality risk of climate change, following equation (3). To do so, we rearrange the agent's first-order conditions and use the conventional definition of the VSL to show that marginal adaptation costs equal the value of marginal adaptation benefits, when evaluated at the optimal level of adaptation $\boldsymbol{b}^*$ and consumption x^*: $\frac{\partial A(\boldsymbol{b}_t^*)}{\partial \boldsymbol{b}} = -VSL_t \frac{\partial \tilde{f}(\boldsymbol{b}_t^*, \boldsymbol{C}_t)}{\partial \boldsymbol{b}}$. That is, representative agents invest in adaptation up to the point where the marginal mortality benefits of further adaptation equal their marginal costs. This simple manipulation of the first-order condition enables us to use marginal adaptation benefits, which we obtain from Section IV's empirical estimates of how warming in the long-run climate lowers mortality's sensitivity to temperature, to infer estimates of marginal adaptation costs.

The total adaptation costs incurred as the climate changes gradually from t_0 to t are recovered by integrating equation (5)'s first-order conditions over time:

$$\begin{aligned} \underbrace{A(\boldsymbol{b}^*(Y_t, \boldsymbol{C}_t)) - A(\boldsymbol{b}^*(Y_t, \boldsymbol{C}_{t_0}))}_{\text{total adaptation costs}} &= \int_{t_0}^{t} \underbrace{\frac{\partial A(\boldsymbol{b}_s^*)}{\partial \boldsymbol{b}} \frac{\partial \boldsymbol{b}_s^*}{\partial \boldsymbol{C}}}_{\substack{\text{marginal} \\ \text{adaptation costs}}} \frac{d\boldsymbol{C}_s}{ds} ds \\ &= \int_{t_0}^{t} \underbrace{-VSL_s \frac{\partial \tilde{f}(\boldsymbol{b}_s^*, \boldsymbol{C}_s)}{\partial \boldsymbol{b}} \frac{\partial \boldsymbol{b}_s^*}{\partial \boldsymbol{C}}}_{\substack{\text{marginal adaptation} \\ \text{benefits}}} \frac{d\boldsymbol{C}_s}{ds} ds. \end{aligned} \tag{6}$$

Equation (6) states that total adaptation costs incurred as the climate changes from t_0 to t equal the integral of marginal adaptation costs in each period (first equality), and that the agent's first-order condition implies that these marginal adaptation costs can be inferred from using the VSL to monetize observable marginal adaptation benefits (second equality). Therefore, estimates of marginal

adaptation benefits can be used to infer total changes in adaptation costs under climate change, even though adaptive investments and their costs are not directly observable.

To empirically estimate total adaptation costs following equation (6), we calculate the following approximation:

$$A(\boldsymbol{b}^*(Y_t, \boldsymbol{C}_t)) - A(\boldsymbol{b}^*(Y_t, \boldsymbol{C}_{t_0})) \approx -\sum_{\tau=t_0+1}^{t} VSL_\tau \underbrace{\left(\frac{\partial \mathrm{E}[\hat{g}]}{\partial TMEAN}\bigg|_{\boldsymbol{C}_\tau, Y_t} \right)}_{\hat{\boldsymbol{\gamma}}_1 \mathrm{E}[\boldsymbol{T}]_\tau} \times (TMEAN_\tau - TMEAN_{\tau-1}) \tag{7}$$

which follows from taking the partial derivative of the estimating equation (equation (4)) with respect to climate to recover the marginal benefits of adaptation, and implementing a discrete-time approximation for the continuous integral. The underbraced object, $\hat{\boldsymbol{\gamma}}_1 \mathrm{E}[\boldsymbol{T}]_\tau$, is the product of the expectation of temperature and the coefficient associated with the interaction between temperature and climate from fitting equation (4): it is the estimated benefits of marginal adaptation.[23] This object is then multiplied by the change in average temperature between each period.[24] Finally, we treat the VSL as a function of income, which evolves as incomes increase over time. Thus, equation (7) represents the sum from t_0 to t of the monetary value of the marginal mortality-related benefits of adaptation in each period, which is equivalent to the sum of marginal mortality-related adaptation costs in each period.

Some intuition may be helpful here. This approach to recovering adaptation costs requires two pieces: (i) estimates of adaptation's marginal benefits (i.e., $\hat{\gamma}\mathrm{E}[\boldsymbol{T}]$); and (ii) the assumption that individuals make all adaptation investments where the benefits exceed the costs and none of the investments where the costs exceed the benefits. The examples of Seattle, WA, and Houston, TX, which have similar incomes but distinct climates, are instructive. Houston has adapted to its hotter climate; we estimate that the

23. The functional form we use to estimate mortality as a function of temperature, climate, and income is $g(\cdot) = \left(\boldsymbol{\gamma}_0 + \boldsymbol{\gamma}_1 TMEAN_t + \boldsymbol{\gamma}_2 \log(GDPpc)_t\right) \boldsymbol{T}_t$. Thus, the partial derivative $\frac{\partial \mathrm{E}[\hat{g}]}{\partial TMEAN}$ equals $\hat{\boldsymbol{\gamma}}_1 \mathrm{E}[\boldsymbol{T}]_\tau$.

24. We assume that individuals use the recent past to form expectations about current temperatures, so this expectation is computed over the prior 15 years with weights that decline in time following a Bartlett kernel, as in Online Appendix E.1.

effect of a 30°C day on the annual > 64 year old mortality rate (relative to a day at 20°C) is ∼15 times larger in Seattle than it is in Houston. Our approach assumes that the costs required to achieve Houston-like protection from hot days must exceed the benefits that Seattle would receive from adopting similar practices. This assumption seems plausible: Houston has an average of 26.3 days $\geqslant$ 30°C annually, compared with 0.02 such days in Seattle, and its air conditioning penetration rate is 100%, while Seattle's is just 27% (Barreca et al. 2016). Put plainly, it appears that the high costs of installing air conditioning exceed its benefits in Seattle, but not in Houston, where it saves lives on many more days per year.

Of course, the climatic difference between Seattle and Houston is nonmarginal. In the limit, the benefits of adaptation in response to a marginal climate difference exactly equal their costs. We can therefore compute the total adaptation costs associated with a nonmarginal change in climate by summing the empirical estimates of the marginal mortality benefits of adaptation over all of the marginal climate changes that together equal the nonmarginal change. In practice, these adaptation cost estimates are calculated annually for each impact region and age group and for the 33 climate models.

The estimates of adaptation costs enable us to develop a complete measure of the full mortality risk of climate change that captures both the benefits and costs of adaptation (equation (3)). Its empirical implementation is:

$$\textit{full mortality risk of climate change} = \underbrace{VSL_t[\,\hat{g}(\boldsymbol{T}_t, TMEAN_t, \log(GDPpc)_t) - \hat{g}(\boldsymbol{T}_{t_0}, TMEAN_{t_0}, \log(GDPpc)_t)]}_{\text{mortality effects of climate change (USD)}}$$

$$+ \underbrace{[A(TMEAN_t, GDPpc_t)\widehat{\ } - \widehat{A}(TMEAN_{t_0}, GDPpc_t)]}_{\text{estimated adaptation costs}}. \tag{3′}$$

Equation (3′) is expressed in dollars, using the VSL to monetize changes in the mortality rate. In some calculations below, we instead present the full mortality risk of climate change in human lives by dividing equation (3′) by the VSL, which is natural because estimated adaptation costs are based on lives that could be saved via adaptation but are not. In these calculations, the adaptation costs are effectively in units of "death equivalents," or the

number of avoided deaths equal in value to the adaptation costs incurred.

A few details of this approach are worth underscoring. First, while equation (6) is derived from the equivalence of adaptation's marginal benefits and marginal costs, total adaptation benefits and costs associated with a nonmarginal change in the climate are not equal. This is because as the climate gradually warms, an impact region's marginal adaptation investment in period t is inframarginal in period $t + 1$, such that each period's total investments can have positive surplus because of investments made in prior periods (see Online Appendix A.3 for details).

Second, while we integrate over changes in climate in equation (6), we hold income fixed at its endpoint value. This is because the goal is to develop an estimate of the additional adaptation expenditures incurred due to the changing climate only. In contrast, changes in expenditures due to rising income will alter mortality risk under climate change, but are not a consequence of the changing climate; therefore they are not included in the calculation of the full mortality risk of climate change.

Third, this revealed-preference approach is purposefully parsimonious so that it can be tightly linked to available data, but such simplification requires several important assumptions. We assume that adaptation costs are a function of technology and do not depend on the climate, so that, for example, people in Seattle can purchase the same air conditioners as people in Houston can. We additionally assume that all individual and societal decisions about adaptation can be captured by the optimizing behavior of a single representative agent in each of the 24,378 regions into which we divide the globe. Further, we assume that $\tilde{f}(\cdot)$ is continuous and differentiable, that markets clear for all technologies and investments represented by the composite good $\boldsymbol{b}$, as well as for the numeraire good x, and that all choices $\boldsymbol{b}$ and x can be treated as continuous. We also assume that neither adaptation investments nor the climate directly enter the utility function, because our focus is limited to the mortality risks of climate change.[25]

25. In an alternative specification detailed in Online Appendix A.5, we allow agents to derive utility both from x and from the choice variables in $\boldsymbol{b}$; for example, air conditioning may increase utility directly, in addition to lowering mortality risk. Under this alternative framework, the costs of adapting to climate change that we can empirically recover, $A(\boldsymbol{b})$, are net of any changes in direct utility benefits or costs. Similarly, a model that assumes that climate enters utility directly would

Perhaps most important, the problem in equation (5) is static. That is, we assume that there is a competitive and frictionless rental market for all capital goods (e.g., air conditioners), so that fixed costs of capital can be ignored, and all rental decisions are contained in $\boldsymbol{b}$. While this assumption rules out complementarities between adaptation decisions made by the representative agent in different time periods by assuming that such complementarities can be accommodated by sellers of adaptation services, accounting for dynamic decision making would necessitate an ambitious extension of the current study, and we leave this to future research.[26]

VI.B. Projections of the Full Mortality Risk of Climate Change, Accounting for Adaptation Benefits and Costs

Table II summarizes the results for the mortality effects of climate change and the full mortality risk of climate change, which accounts for adaptation benefits and costs, at the end of the century. The columns follow equations (2′)–(3′). Specifically, column (1) reports the mortality effects of climate change without income growth or adaptation (equation (2a′)). Columns (2) and (3) show the change in the mortality effects of climate change due to the benefits of income growth and climate adaptation, respectively (differences between equations (2′), (2a′), and (2b′)); both tend to reduce mortality effects, so the entries are negative. Column (4) presents estimates of the mortality effects of climate change (equation (2′)) and is equal to the sum of columns (1)–(3). Column (5) shows adaptation costs in units of death equivalents, following the calculation in equation (7). Finally, columns (6) and (7) show the full mortality risk of climate change (equation (3′)), measured in deaths per 100,000 and monetized as a proportion of total global GDP in 2100, respectively.

---

also lead to any adaptation costs associated with the direct effects of climate change being "netted out" in estimated adaptation costs.

26. For example, the central contribution of Lemoine (2018) is to incorporate complementarity in adaptation actions across periods in a standard climate change effect model. This article analyzes only a two-period complementarity, yet estimation in our context would require accurate weather forecast data for all locations and years in our estimating sample, a binding constraint in many countries. It is also worth noting that the quantitative effects of adding dynamic decision making in Lemoine (2018) were minor, changing the end-of-century estimated losses to U.S. agriculture due to climate change from 47% under a static model to 50% under a dynamic model (see table 2).

TABLE II

GLOBAL AND REGIONAL ESTIMATES OF THE FULL MORTALITY RISK OF CLIMATE CHANGE IN 2100 (HIGH-EMISSIONS SCENARIO, RCP8.5)

	No income growth or adaptation	Benefits of income growth	Benefits of climate adaptation	Mortality effects of climate change	Costs of climate adaptation	Full mortality risk of climate change	
	Eq. (2a′) deaths/100k (1)	Eq. (2b′)–Eq. (2a′) deaths/100k (2)	Eq. (2′)–Eq. (2b′) deaths/100k (3)	Eq. (2′) deaths/100k (4)	Eq. (7) deaths/100k (5)	Eq. (3′) deaths/100k (6)	% of GDP (7)
Panel A: Global estimates							
Mean effects	220.6	−116.5	−31.0	73.1	11.7	84.8	3.2
Full uncertainty IQR	[76.4, 258.8]	[−149.4, −39.2]	[−60.1, 3.8]	[5.6, 101.4]	[0.2, 19.4]	[17.4, 116.4]	[−5.4, 9.1]
Panel B: Regional estimates							
China	112.0	−81.8	−28.8	1.4	17.7	19.1	1.9
United States	14.8	−13.2	−1.8	−0.2	10.2	10.1	1.0
India	334.4	−248.2	−25.6	60.6	2.1	62.7	6.0
Pakistan	589.1	−161.7	−105.0	322.4	53.6	376.0	27.5
Bangladesh	382.5	−89.3	−79.3	213.8	34.7	248.5	18.5
Europe	−14.3	−6.2	−74.8	−95.5	90.8	−4.7	0.1
Sub-Saharan Africa	232.5	−77.4	−34.5	121.3	10.5	131.8	8.4

Notes. The table shows projections of the mortality effects of climate change and the full mortality risk of climate change across all age categories. Mean estimates are averages across a set of Monte Carlo simulations accounting for both climate model and statistical uncertainty. In Panel A, brackets indicate the interquartile range (IQR). Columns (1)–(4) are computed using the three measures of the mortality effects of climate change detailed in Section V, all in units of deaths per 100,000. Column (1) (equation (2a′)): mortality effects of climate change without benefits of income or adaptation to climate change. Column (2) (equation (2b′) − equation (2a′)): benefits of income growth. Column 3 (equation (2′) − equation (2b′)): benefits of adaptation to climate change. Column 4 (equation (2′), equal to the sum of columns 1–3): mortality effects of climate change. Column 5 shows the mortality-related costs of adaptation inferred using a revealed-preference approach (equation (7) divided by the VSL), measured in death equivalents. Columns (6) and (7) show the full mortality risk of climate change (equation (3′)), measured in deaths per 100,000 (column (6)) and represented as % of 2100 GDP (column (7)) using an age-adjusted value of the U.S. EPA VSL with an income elasticity of one applied to all impact regions. Column (6) is equivalent to the sum of columns (4) and (5). The signs in columns (6) and (7) can differ because of different relative weights on heterogeneous mortality risks across regions and age groups. All estimates shown rely on the RCP8.5 emissions scenario and the SSP3 socioeconomic scenario. Online Appendix Table F.2 shows equivalent results for SSP3 and RCP4.5 and details the regional definitions for Europe and sub-Saharan Africa.

1. *Global Estimates of the Full Mortality Risk of Climate Change.* Table II, Panel A shows mean estimates for the globe, averaging over a set of Monte Carlo simulations accounting for both climate and econometric uncertainty. The interquartile ranges across simulation runs are in brackets. Column (6) shows that, on average, the estimated full mortality risk of climate change (equation (3′)) is projected to equal ∼85 deaths per 100,000 under RCP8.5 by 2100 (Online Appendix Figure F.2 shows annual results over the century and Online Appendix Table F.2 shows results for RCP4.5). Of this full mortality risk, climate adaptation costs are estimated at ∼12 death equivalents per 100,000 (column (5)), while increases in mortality rates account for the remaining 73 deaths per 100,000 (column (4)). It is noteworthy that the estimated global average benefits of adaptation (column (3); 31 deaths per 100,000) exceed the costs of these adjustments, revealing an adaptation surplus of 19 deaths per 100,000.

Table II, column (7) reports that the monetized full mortality risk of climate change at the end of the century is substantial. For example, under RCP8.5, it amounts to 3.2% of global GDP in 2100, with an interquartile range of [−5.4%, 9.1%]. Under RCP4.5 (shown in Online Appendix Table F.2), this value falls to 0.6% [−3.9%, 4.6%] of global GDP, revealing the significant benefits of policies to reduce emissions. The uncertainty around these estimates is also meaningful. As shown in Online Appendix Table F.1, climate and econometric uncertainty contribute roughly equally to the overall variance in the full mortality risk of climate change when it is measured in death equivalents (column (6a)). However, econometric uncertainty becomes the predominant source of uncertainty when deaths are converted to dollars, reflecting that these two sources of uncertainty differentially affect low- and high-income populations (whose deaths are valued differently based on heterogeneous VSLs). Section VII shows that accounting for this uncertainty with standard assumptions about the degree of individuals' risk aversion substantially increases the estimated welfare loss from climate change.

These results suggest that the mortality-related damages from climate change are much greater than had previously been understood. For instance, the full mortality risk of climate change amounts to ∼49%–135% of the damages reported for all sectors of the economy in FUND, PAGE, and DICE at the end of the century. Under RCP4.5, the full mortality risk of climate change amounts

to 32%–61% of the damages from DICE and PAGE, while damages from FUND are negative at RCP4.5 levels of warming.[27]

The results in this and the previous section have relied on a single benchmark emissions and socioeconomic scenario (RCP8.5, SSP3). Online Appendix F reports on the sensitivity of these results to alternative choices about the economic and population scenario, the emissions scenario, and assumptions regarding the rate of adaptation. These exercises underscore that the projected impacts of climate change over the remainder of the twenty-first century depend on difficult-to-predict factors such as policy, technology, and demographics. However, in all SSP scenarios, and an alternative projection in which the rate of adaptation is deterministically slowed, the average estimate of the full mortality risk due to climate change is positive (under both RCPs) and steadily increasing (under RCP8.5) throughout the twenty-first century.

2. *Unequal Distribution of the Full Mortality Risk of Climate Change.* Table II, Panel B displays mean estimates of the end-of-century mortality effects of climate change and the full mortality risk of climate change for key select countries and regions of the world. These results indicate that the full mortality risk of climate change varies substantially around the world. Notably, monetized estimates in column (7) are very high in some regions, such as Pakistan and Bangladesh, where effects amount to 27.5% and 18.5% of GDP, respectively.[28] Panel B also shows that the share of the full mortality risk that is attributable to actual deaths (first

27. To conduct this comparison, we use the damage functions reported for each IAM in the Interagency Working Group on Social Cost of Carbon (2010), which are indexed against warming relative to the preindustrial climate. We evaluate each damage function at the mean end-of-century warming (4°C for RCP8.5 and 1.8°C for RCP4.5) across the SMME climate model ensemble used in our analysis, after adjusting warming to align preindustrial temperature anomalies from the IAMs with the anomalies relative to 2001–2010 from our analysis (Lenssen et al. 2019). We note that these leading IAMs use different socioeconomic scenarios and climate models than those used throughout this article.

28. Note that Table II indicates that for Europe, the full mortality risk of climate change as measured in deaths per 100,000 (column (6)) is negative, while it is positive when measured in % of GDP (column (7)). This is because throughout much of Europe, climate change leads to lives being saved due to fewer extremely cold days, particularly for the > 64 age group. Under the valuation approach shown in Table II, an age-adjusted VSL is used, which lowers the relative weight placed on these lives saved in the older age group, as compared with increased mortality risk due to hot days in other age groups.

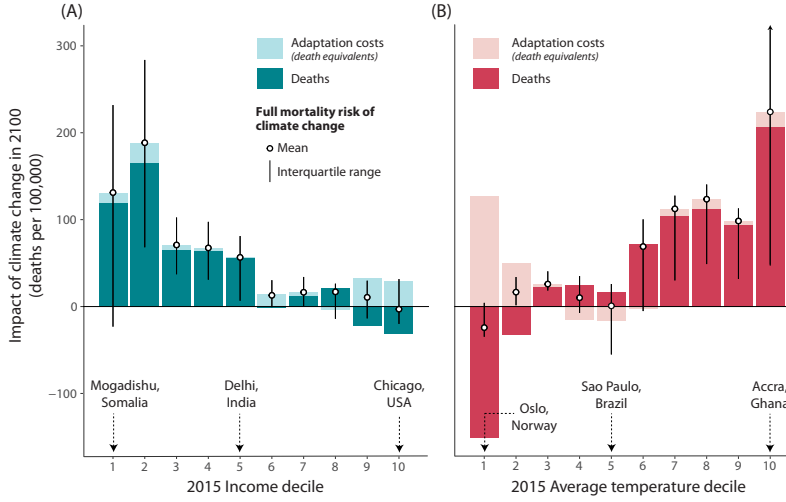

FIGURE VI

Climate Change Effects and Adaptation Costs are Correlated with Present-Day Income and Climate

Figure shows mortality effects of climate change in 2100 (RCP8.5, SSP3) against deciles of 2015 per capita income (Panel A) and average annual temperature (Panel B). Dark bars indicate mean estimates of the mortality effects of climate change (following equation (2′)), and light shading indicates mean estimates of changes in adaptation costs, measured in death equivalents (equation (7) divided by the VSL). For all bars, means are taken across impact regions falling into the corresponding decile of income or climate and across Monte Carlo simulations that account for econometric and climate model uncertainty. Black outlined circles indicate the mean estimate of the full mortality risk of climate change (following equation (3′)), which is the sum of deaths and adaptation costs, and black vertical lines indicate the interquartile range of the distribution across impact regions in each decile. The income and average temperature deciles are calculated across 24,378 global impact regions and are population weighted using 2015 population values.

term in equation (3′), column (4)) versus compensatory investments (second term in equation (3′), column (5)) differs across regions. Some locations suffer large increases in mortality rates, such as India, where 97% of the full mortality risk of climate change is attributable to rising death rates. Other regions avoid excess mortality through expensive adaptation. For example, the United States is projected to benefit from a small decline in the mortality rate of −0.2 deaths per 100,000 at end of century but is also projected to incur adaptation costs amounting to 10 death equivalents per 100,000.

To visualize these distributional consequences, Figure VI plots the mortality effects of climate change in 2100 (dark

bars), as well as estimated adaptation costs (light bars), against deciles of present-day income (Panel A) and present-day average temperature (Panel B). These results reveal that the magnitude and composition of the full mortality risk of climate change are strongly correlated with current incomes and climate. Panel A shows that the share of the full mortality risk of climate change that is due to adaptation costs is higher at higher incomes, indicating that wealthier locations are projected to pay for future adaptive investments, while such costs are predicted to be much smaller in poor parts of the world. In contrast, mortality rates are projected to increase much more dramatically in today's poor countries, indicating that climate effects in these places will largely take the form of people living shorter lives. Further, the full mortality risk of climate change (shown in black and white circles) is still borne disproportionately by regions that are poor today. Finally, there is substantial variance across impact regions in each income decile, as shown by the interquartile range indicated by the vertical blank line, underscoring the importance of geographic resolution in projecting climate impacts.

A similar figure in Panel B demonstrates that the hottest locations today suffer the largest projected increases in death rates, whereas the coldest are estimated to pay the highest adaptation costs. It is also evident that the full mortality risk of climate change is highest in today's hottest regions.

VII. The Mortality Partial Social Cost of Carbon

This section uses the estimates of the full mortality risk of climate change to monetize the mortality-related social cost generated by emitting a marginal ton of CO_2. This calculation represents the component of the total SCC that is mediated through excess mortality, but it leaves out adverse effects in other sectors of the economy, such as reduced labor or agricultural productivity. Hence, it is a mortality partial SCC.

VII.A. Definition: The Mortality Partial SCC

The mortality partial SCC at time t is defined as the marginal social cost from the change in mortality risk imposed by the emission of a marginal ton of CO_2 in time period t. For a discount rate

δ, the mortality partial SCC is:

$$(8)\quad \textit{mortality partial } SCC_t \ \ (\textit{dollars}) = \int_t^{\infty} e^{-\delta(s-t)} \frac{dD_s(\boldsymbol{C}_s)}{d\boldsymbol{C}} \frac{\partial \boldsymbol{C}_s}{\partial E_t} ds,$$

where $D_s(\boldsymbol{C}_s)$ represents a "damage function" describing the full mortality risk of climate change (inclusive of adaptation benefits and costs) in time period s, as a function of the global climate $\boldsymbol{C}$ (Nordhaus 1992; Hsiang et al. 2017), and where E_t represents total global greenhouse gas emissions in period t. $D_s(\cdot)$ varies over time, s, because the mortality sensitivity of temperature and total monetized effects of climate change evolve over time due to changes in per capita income, the climate, and the underlying population. Thus, the damages from a marginal change in emissions will vary depending on the year in which they are evaluated. In practice, we approximate equation (8) by combining empirically grounded estimated damage functions $D_s(\cdot)$ with climate model simulations of the effect of a small change in emissions on the global climate, that is, $\frac{\partial \boldsymbol{C}_s}{\partial E_t}$.

Expressing the mortality partial SCC using a damage function has three key practical advantages. First, the damage function represents a parsimonious, reduced-form description of the otherwise complex dependence of global mortality damages on the global climate. Second, as we demonstrate below, it is possible to empirically estimate damage functions from the climate change projections described in Section VI. Finally, because they are fully differentiable, empirical damage functions can be used to compute marginal damages caused by an emissions pulse released in year t by differentiation. The construction of these damage functions, as well as the implementation of the mortality partial SCC, are detailed in the following subsections.

VII.B. Constructing Damage Functions for Mortality Risk from Climate Change

There are two key components of a damage function for mortality risk. First, the change in global mean surface temperature, $\Delta GMST_{rmt}$ indicates the overall magnitude of warming for each emissions scenario r, climate model m, and year t.[29] Second,

29. Our estimates of the full mortality risk of climate change are calculated relative to a baseline of 2001–2010. Therefore, we define changes in global mean surface temperature ($\Delta GMST$) as relative to this same period. Note that the

total monetized losses due to changes in mortality risk, inclusive of adaptation benefits and costs, D_{irmt}, captures total mortality damages for a given level of warming. We compute this value by summing projected estimates of the monetized full mortality risk of climate change across all 24,378 global impact regions, separately for each draw i of the uncertain parameters recovered from estimation of the mortality-temperature relationship in equation (4), emissions scenario r, climate model m, and year t. Therefore, for a given value of $\Delta GMST_{rmt}$, there is variation in damages D_{irmt} due to econometric uncertainty captured by simulation runs i and differential spatial distribution of warming across climate model m.

There are some important methodological differences in how we estimate the relationship between damages D_{irmt} and warming $\Delta GMST_{rmt}$ for years before versus after 2100, because of differences in the source of climate projections pre- and post-2100 and the absence of readily available socioeconomic projections after 2100 (see Section III and Online Appendix B.2 for details). This subsection details these differences and explains the approach to account for damage function uncertainty.

1. *Computing Damage Functions through 2100.* For each year t from 2020 to 2097, we estimate a set of quadratic damage functions that relate the global full mortality risk of climate change (D_{irmt}) to the magnitude of global warming ($\Delta GMST_{rmt}$):

$$D_{irmt} = \alpha + \psi_{1,t}\Delta GMST_{rmt} + \psi_{2,t}\Delta GMST_{rmt}^2 + \varepsilon_{irmt}. \tag{9}$$

Specifically, we construct the damage function separately for each year t by combining all 9,750 Monte Carlo simulation runs within a five-year window centered on t and estimate the regression in equation (9).[30] This approach allows the recovered damage function $D_t(\Delta GMST)$ to evolve flexibly over the century. We note that pre-2100 damage functions are indistinguishable if we use a third-, fourth-, or fifth-order polynomial, and Online Appendix H.4

$\Delta GMST_{rmt}$ will vary across climate models, due to the complex interaction of many physical elements in each model, including the equilibrium climate sensitivity, a number that describes how much warming is associated with a specified change in greenhouse gas emissions.

30. Because the projections in Section VI end in 2100, 2097 is the last year for which a centered five-year window of estimated damages can be constructed, and therefore is the last year for which we estimate equation (9).

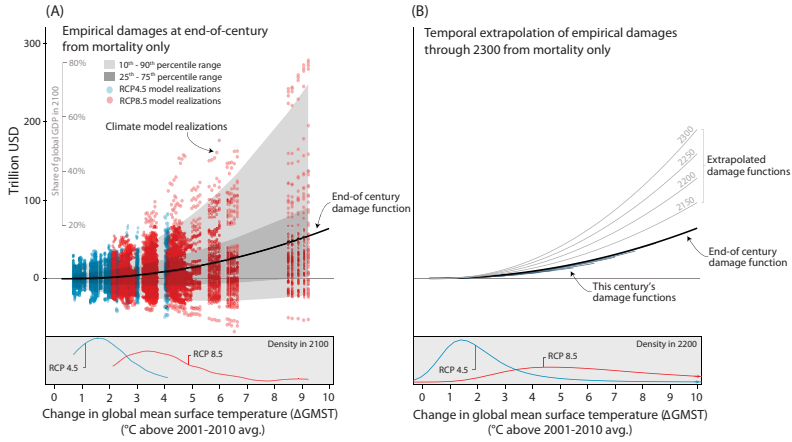

FIGURE VII

Empirically Derived Mortality-Only Damage Functions

Both panels show damage functions relating empirically derived total global mortality damages to anomalies in global mean surface temperature (ΔGMST) under socioeconomic scenario SSP3. In Panel A, each point indicates the full mortality risk of climate change in a single year (ranging from 2095 to 2100) for a single simulation of a single climate model, accounting for both costs and benefits of adaptation. The solid black line is the quadratic damage function estimated through these points. The distribution of temperature anomalies at end of century (2095–2100) under two emissions scenarios across our 33 climate models is in the bottom panel. In Panel B, the end-of-century damage function is repeated. Damage functions are shown for every 10 years before 2100, each of which is estimated analogously to the end-of-century damage function and is shown covering the support of ΔGMST values observed in the SMME climate models for the associated year. Our projection results compute the full mortality risk of climate change only through 2100, due to limited availability of climate and socioeconomic projections for years beyond that date. To capture effects after 2100, we extrapolate observed changes in damages over the twenty-first century to generate time-varying damage functions through 2300. The resulting damage functions are shown for every 50 years post-2100, each of which is extrapolated. The distribution of temperature anomalies around 2200 (2181–2200) under two emissions scenarios using the FAIR simple climate model is in the bottom panel. To value lives lost or saved, in both panels we use the age-varying U.S. EPA VSL and an income elasticity of 1 applied to all impact regions.

shows that the mortality partial SCC is similar when a cubic functional form is used.

Figure VII, Panel A illustrates the procedure for the end-of-century damage function. Each data point plots a value of D_{irmt} from an individual Monte Carlo simulation (vertical axis) against the corresponding value of $\Delta GMST_{rmt}$ (horizontal axis), where scatter points for years $t = 2095$ through $t = 2100$ are

shown. Individual points represent simulation runs from both the high-emissions scenario (r = RCP8.5) and from the low-emissions scenario (r = RCP4.5). The estimated end-of-century damage function predicts total (undiscounted) mortality damages of \$7.8 trillion when evaluated at median warming under RCP8.5 (+3.7°C relative to 2001–2010). For RCP4.5, median warming is 1.6°C, with corresponding predicted damages of \$1.2 trillion. Analogous curves are constructed for all years, starting in 2020.

2. *Computing Post-2100 Damage Functions.* Even with standard discount rates, a meaningful fraction of the present discounted value of damages from the release of CO_2 today will occur after 2100 (Kopp and Mignone 2012), so it is important to develop post-2100 damage functions. To do so, we develop a method to extrapolate changes in the damage function beyond 2100 using the observed evolution of damages near the end of the twenty-first century. The motivating principle of the extrapolation approach is that these observed changes in the shape of the damage function near the end of the century provide plausible estimates of future damage function evolution after 2100. To execute this extrapolation, we pool values D_{irmt} from 2085–2100 and estimate a quadratic model similar to equation (9), but interacting each term linearly with year t.[31] This allows us to estimate a damage surface as a parametric function of year, which can then be used to predict extrapolated damage functions for all years after 2100 (see Online Appendix G for details).

Figure VII, Panel B illustrates damage functions every 10 years before 2100, as well as extrapolated damage functions for 2150, 2200, 2250, and 2300. In dollar terms, these extrapolated damages continue to rise after 2100, suggesting larger damages for a given level of warming. This finding comes directly from the estimation of equation (9), which found that in the latter half of the twenty-first century, mortality damages are larger when they occur later, holding constant the degree of warming. This finding that mortality damages rise over time reflects several countervailing forces. On the one hand, damages are larger in later years because there are larger and older populations with higher VSLs due to rising incomes.[32] On the other hand, damages are smaller

31. We use 2085–2100 because the time evolution of damages becomes roughly linear conditional on ΔGMST by this period.

32. In SSP3, the share of the global population in the > 64 age category rises from 8.2% in 2015 to 16.2% in 2100.

in later years because populations are better adapted because of higher incomes and a slower rate of warming, enabling gradual adaptation. The results suggest the former dominates by end of century, causing damages to trend upward by 2100.

3. *Accounting for Uncertainty in Damage Function Estimation.* As discussed, there is substantial uncertainty in the projected full mortality risk of climate change due to econometric uncertainty and climate uncertainty. The approach described above details the estimation of a damage function using the conditional expectation function through the full distribution of simulation results. We also estimate a set of quantile regressions to capture the full distribution of simulated mortality effects.[33] Just as before for the mean damage function, extrapolation past 2100 is accomplished using a linear time interaction, estimated separately for each quantile. In the sections that follow, these quantiles characterize uncertainty in the mortality partial SCC estimates. Thus, central estimates of the mortality partial SCC use the mean regression from equation (9), while ranges incorporating damage uncertainty use the full set of time-varying quantile regressions.

VII.C. Computing Marginal Damages from a Marginal Carbon Dioxide Emissions Pulse

We empirically approximate the mortality partial SCC from equation (8) for emissions that occur in 2020 as:

$$\begin{aligned} &\textit{mortality partial SCC}_{2020} \\ &\approx \sum_{t=2020}^{2300} e^{-\delta(t-2020)} \frac{\partial \hat{D}_t(\Delta GMST)}{\partial \Delta GMST} \frac{d\Delta GMST_t}{dCO2_{2020}}, \end{aligned} \tag{10}$$

where $\Delta GMST$ approximates the multidimensional climate vector $\boldsymbol{C}$, and changes in CO_2 represent changes in global emissions $\boldsymbol{E}$.[34] In addition, we assume that discounted damages from an emissions pulse in 2020 become negligible after 2300, and we approximate the integral in equation (8) with a discrete sum using increments of one year. The values $\frac{\partial \hat{D}_t(\Delta GMST)}{\partial \Delta GMST}$ are the marginal

33. We estimate a damage function for every fifth percentile from the 5th to the 95th.

34. We use CO_2 to represent changes in all global greenhouse gas (GHG) emissions because it is the most abundant GHG and the warming potential of all other GHGs are generally reported in terms of their CO_2 equivalence.

global damages in each year t that occur as a result of this small change in all future global temperatures; they are computed using the damage functions described in the last subsection. The term $\frac{d\Delta GMST_t}{dCO2_{2020}}$ is the increase in $\Delta GMST$ that occurs in each year t along a baseline climate trajectory as a result of a marginal unit of emissions in 2020, which we approximate with small pulse of CO_2 emissions.

Because it is computationally infeasible to compute this value and account for uncertainty about the physical magnitude and timing of warming for all 33 climate models in the SMME, we use an alternative global climate model to estimate $\frac{d\Delta GMST_t}{dCO2_{2020}}$. In particular, we use the Finite Amplitude Impulse Response (FAIR) simple climate model to calculate $\Delta GMST_t$ trajectories for emissions scenarios RCP4.5 and RCP8.5, with and without an exogenous "pulse" of 1 gigaton C (equivalent to 3.66Gt CO_2) in the year 2020, the smallest emission quantity for which a warming signal can be separated from noise in the FAIR climate model. In FAIR, this emissions pulse perturbs the trajectory of atmospheric CO_2 concentrations and $\Delta GMST$ for 2020–2300, with dynamics that are influenced by the baseline RCP scenario.

We then predict damages $\hat{D}_t(\Delta GMST_t)$ for $\Delta GMST$ values from the "RCP + pulse" simulation and difference them from predicted damages for $\Delta GMST$ values from the baseline "RCP only" simulation for each emissions scenario. The resulting damages due to the pulse are converted into US$ per metric ton CO_2. There is naturally uncertainty in these $\Delta GMST$ trajectories, and our approach accounts for uncertainty associated with four key parameters of the FAIR model. This approach, detailed in Online Appendix G, ensures that the distribution of warming responses that we use to generate partial SCC values matches the corresponding distributions from the IPCC Assessment Report 5 (AR5).

Figure VIII graphically depicts the difference between the RCP + pulse and baseline RCP trajectories for four key outcomes. The pulse in emissions is shown in Panel A. Its influence on CO_2 concentrations is reported in Panel B; the immediate decline followed by a century-long increase is largely due to dynamics involving the ocean's initial storage and subsequent release of emissions. Panel C displays the resulting change in temperature, which makes clear that a pulse today will influence temperatures even three centuries later. The solid lines are median estimates, while the shaded area in Panels B and C depicts the interquartile range of each year's outcome, reflecting uncertainty about the climate system (see Online Appendix G for details).

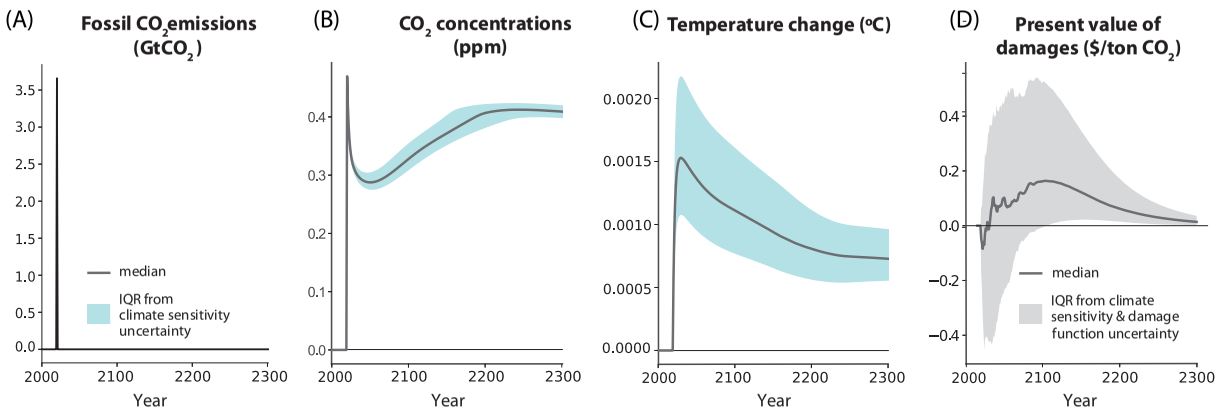

FIGURE VIII

Change in Emissions, Concentrations, Temperature, and Damages Due to a Marginal Emissions Pulse in 2020

Panel A shows a 1 GtC emissions pulse (equivalent to 3.66 Gt CO_2) in 2020 for emissions scenario RCP8.5. Panel B displays the effect of this pulse on atmospheric CO_2 concentrations, relative to the baseline. In Panel C, the effect of the pulse of CO_2 on temperature is shown where the levels are anomalies in global mean surface temperature (GMST) in Celsius. In Panels B and C, shaded areas indicate the interquartile range due to climate sensitivity uncertainty, and solid lines are median estimates. Panel D shows the change in discounted mortality-related damages over time due to a 1 Gt pulse of CO_2 in 2020 under socioeconomic scenario SSP3, as estimated by our empirically derived damage functions, using a 2% annual discount rate and the age-varying U.S. EPA VSL with an income elasticity of 1 applied to all impact regions. The shaded area indicates the interquartile range due to climate sensitivity and damage function uncertainty, and the solid line is the median estimate.

Panel D plots the discounted (2% discount rate) stream of damages due to this marginal pulse of emissions. The temporal pattern of the present value of mortality damages reflects several factors, including the nonlinearity of the damage function (e.g., Figure VII), the discount rate, and the dynamic temperature response to emissions (Panel C). The peak present value of annual damages from a ton of CO_2 emissions are \$0.16 in 2104; by 2277, annual damages are always less than \$0.02. It is noteworthy that about two-thirds of the present value of damages occur after 2100. The shaded area represents the interquartile range of each year's outcome, reflecting uncertainty in the climate system and in the damage function. RCP4.5 results are shown in Online Appendix Figure G.5, and additional details are in Online Appendix G.

VII.D. Estimates of the Mortality Partial SCC

Table III reports mortality partial SCC estimates. The columns apply four different annual discount rates—two used in prior estimates of the SCC (3% and 5%) (Interagency Working Group on Social Cost of Carbon 2010), and two lower rates that align more closely with recent global capital markets (1.5% and 2%) (Board of Governors of the U.S. Federal Reserve System 2020). Both panels use the U.S. EPA's VSL of \$10.95 million (2019 US\$), transformed into value per life-year lost and adjusted for cross-sectional variation in incomes among contemporaries and for global income growth (see Online Appendix H.1 for details). We emphasize this age-varying VSL approach because standard economic reasoning implies that valuation of life lost should vary by age (Murphy and Topel 2006; Jones and Klenow 2016), but Online Appendix H presents results under a wide range of additional valuation scenarios, including an age-invariant VSL, an age adjustment that uses age-specific values per life-year from Murphy and Topel (2006), an alternative VSL of \$2.39 million (2019 US\$) from Ashenfelter and Greenstone (2004),[35] and an approach where the VSL is adjusted only based on global average income such that the lives of contemporaries are valued equally, regardless of their relative incomes. The central estimates in Table III use the median values of FAIR's four key parameter distributions

35. See Online Appendix Table H.1 for a comparison of these VSL values with values from the OECD, which are higher than Ashenfelter and Greenstone (2004), but lower than the U.S. EPA's VSL.

TABLE III

ESTIMATES OF THE MORTALITY PARTIAL SOCIAL COST OF CARBON (SCC)

	Annual discount rate			
	$\delta = 1.5\%$ (1)	$\delta = 2\%$ (2)	$\delta = 3\%$ (3)	$\delta = 5\%$ (4)
Panel A: Mortality partial SCC				
Moderate-emissions scenario (RCP4.5)	28.5	17.1	7.9	2.9
Full uncertainty IQR	[−35.6, 88.5]	[−24.7, 53.6]	[−15.2, 26.3]	[−8.5, 11.5]
High-emissions scenario (RCP8.5)	66.4	36.6	14.2	3.7
Full uncertainty IQR	[−2.8, 126.5]	[−7.8, 73.0]	[−11.4, 32.9]	[−8.9, 13.0]
Panel B: Alternative approaches to calculating the mortality partial SCC				
Excluding adaptation costs (RCP8.5)				
Central estimate	66.9	37.7	15.1	4.1
Full uncertainty IQR	[−3.1, 114.6]	[−6.7, 66.4]	[−9.6, 29.8]	[−8.2, 11.5]
Accounting for risk aversion (RCP8.5)				
Central estimate (risk neutral)	88.4	47.7	17.2	3.7
Certainty equivalent (risk averse)	375.3	192.4	59.2	8.6

Notes. In both panels, an income elasticity of 1 is used to scale the U.S. EPA VSL value (alternative values using the VSL estimate from Ashenfelter and Greenstone (2004) are shown in Online Appendix H). All regions thus have heterogeneous valuation, based on local income. All estimates use an age adjustment that values deaths by the expected number of life-years lost, using an equal value per life-year (see Online Appendix H.1 for details and Online Appendix H.2 for alternative calculations that allow the value of a life-year to vary with age, based on Murphy and Topel 2006). All SCC values are for 2020, measured in PPP-adjusted 2019 US$, and are calculated from damage functions estimated from projected results under the socioeconomic scenario SSP3 (alternative values using other SSP scenarios are shown in Online Appendix H). Panel A shows estimates of the mortality partial SCC that include both the benefits and costs of adaptation, as inferred using the revealed-preference framework outlined in Section VI.A. Panel B shows estimates derived from two alternative approaches to calculating the mortality partial SCC. The first two rows include the benefits of adaptation but exclude estimated adaptation costs. The second two rows follow Nath et al. (2022), who use standard calibrations of risk aversion to construct certainty-equivalent mortality partial SCCs using the damage functions estimated in this article. In all panels, central estimates rely on the median values of the four key input parameters into the climate model FAIR and a conditional mean estimate of the damage function. The uncertainty ranges are interquartile ranges including climate sensitivity uncertainty and damage function uncertainty (see the main text and Online Appendix G for details).

(see Online Appendix G) and the mean global damage function. Interquartile ranges (IQRs) are reported, reflecting uncertainty in climate sensitivity and in the damage function. All values represent the global sum of each impact region's MWTP today to avoid the release of an additional metric ton of CO_2 in 2020.

Panel A reports estimates of the mortality partial SCC, including the benefits and costs of adaptation. Our preferred estimates use a discount rate of $\delta = 2\%$ (column (2)), which we highlight because it conservatively reflects changes in global capital markets over the last several decades (Carleton and Greenstone forthcoming).[36] Under this approach, the mortality partial SCC is \$17.1 for the moderate-emissions scenario and \$36.6 for the high-emissions scenario. The associated IQRs are [−\$24.7, \$53.6] and [−\$7.8, \$73.0], respectively, highlighting the uncertainty in the SCC. The discount rate's key role in determining the mortality partial SCC is evident when comparing estimates across columns. When following the U.S. government's preference for an age-invariant VSL and using $\delta = 2\%$, the mortality partial SCC is \$14.9 [−\$21.2, \$63.5] for the moderate-emissions scenario and \$65.1 [−\$3.0, \$139.0] for the high-emissions scenario (see Online Appendix Table H.2).[37]

Some features of these results are worth underscoring. First, mortality partial SCC estimates for RCP4.5 are systematically lower than RCP8.5 primarily because the damage function is convex, so marginal damages increase in the high-emissions scenario. Second, Online Appendix H decomposes the uncertainty in the partial SCC into a component driven by climate uncertainty and a component driven by uncertainty in the damage function. Whereas damage function uncertainty tends to dominate under the moderate-emissions scenario, climate uncertainty is dominant under the high-emissions scenario for some valuation approaches. Third, Online Appendix H also presents results for a

36. While the Interagency Working Group on Social Cost of Greenhouse Gases (2016) recommends a discount rate of 3% based on the real 10-year Treasury rate calculated in 2003, this estimate is now dated. For example, the average 10-year Treasury Inflation-Indexed Security from 2003 to present is just 1.01% (Board of Governors of the U.S. Federal Reserve System 2020; Carleton and Greenstone forthcoming).

37. As detailed in Online Appendix H.2, age adjusting the valuation of mortality rates, which down-weights the valuation of the oldest age group, has an ambiguous influence on the SCC, as this group is more vulnerable both to heat and to cold.

variety of sensitivity analyses. For example, Online Appendix Table H.5 reveals that endogenizing effects of climate change on income growth based on prior literature (Burke, Hsiang, and Miguel 2015), as opposed to relying on an exogenous socioeconomic trajectory as in Table III, has only a small effect on our mortality partial SCC results. Similarly, Online Appendix Table H.6 demonstrates that replacing the extrapolation of damage functions to years beyond 2100 with a damage function frozen at its 2100 shape for all years 2101–2300 lowers our central estimate of the mortality partial SCC by 21%. This indicates that damage function extrapolation has a relatively modest impact on our partial SCC estimates, due partly to the important role of discounting. Further, Online Appendix Tables H.2– H.7 report estimates based on multiple alternative valuation approaches and socioeconomic scenarios. Naturally, the resulting SCC estimates vary under different valuation assumptions and baseline socioeconomic trajectories, and we point readers to these specifications for a more comprehensive set of results.

Panel B reports two sets of estimates that rely on alternative approaches to calculating the mortality partial SCC. The first two rows show mortality partial SCCs that include the benefits of adaptation but exclude estimated adaptation costs. With $\delta = 2\%$, we estimate that the mortality partial SCC amounts to \$37.7 [−\$6.7, \$66.4] when using this approach in the high-emissions scenario.[38]

The third and fourth rows in Panel B address the large uncertainty in the mortality partial SCC by using standard calibrations of risk aversion to estimate certainty-equivalent mortality partial SCCs. This exercise is important because the distribution of partial SCCs is right skewed with a long right tail, largely due to the

38. This small increase in the partial SCC when compared to Panel A arises from adaptation savings in temperate regions of the world that spend less protecting themselves against cold-day mortality risk under a warmer climate. On net, under our preferred valuation approach, these savings outweigh the positive adaptation costs experienced in other regions because temperate regions have relatively high VSLs, and we estimate low future adaptation costs in hot locations that are already well adapted today. This leads to a small decline in the mortality partial SCC when adaptation costs are included. However, the finding that aggregate global adaptation costs are generally negative when measured in dollars depends on how mortality risk is monetized into dollars because we estimate highly heterogeneous adaptation costs across age groups and regions (see Figure VI). For example, global monetized adaptation costs are generally positive when an age-invariant VSL is used.

convexity of the damage function (e.g., see Figure VII) and the skewness of the climate sensitivity distribution (see Online Appendix Figure G.2). For example, the 95th and 99th percentiles of the mortality partial SCC shown in Table III, Panel B for RCP8.5 with $\delta = 2\%$ are \$290.3 and \$704.1, respectively. Although a full treatment of risk is beyond the scope of this article, here we follow Nath et al. (2022) in estimating a certainty-equivalent mortality partial SCC. Importantly, multiple aspects of the Nath et al. (2022) partial SCC calculation differ from this article's, making the resulting SCCs not directly comparable to those in Panel A.[39] Consequently, the third row reports the risk-neutral partial SCC estimate from Nath et al. (2022), which is the Nath et al. (2022) equivalent of the values in Panel A, while the last row reports the certainty-equivalent value.[40] The key finding of this exercise is that valuing uncertainty greatly increases the estimated mortality partial SCC. Using the preferred 2% discount rate with the RCP8.5 emissions scenario, the certainty-equivalent value is approximately four times larger than the directly comparable risk-neutral estimate. These findings empirically corroborate earlier theoretical work highlighting the importance of valuing uncertainty in SCC calculations (e.g., Traeger 2014).

VIII. Limitations

As the article has detailed, the mortality risk changes from climate change and the mortality partial SCC have many factors. We have tried to probe the robustness of the results to each of them, but there are three issues that merit special attention when interpreting the results, because they are outside the scope of the analysis.

VIII.A. Migration Responses

The estimates in the article do not reflect the possibility of migration responses to climate change. If migration were costless,

39. For example, when compared to this article's analysis, Nath et al. (2022) use a more restrictive approach to extrapolating damage functions beyond 2100, estimate damage functions without a constant term, and rely on a smaller set of climate sensitivity parameters, among other differences.

40. The certainty-equivalent estimates rely on a constant relative risk aversion utility function with a coefficient of relative risk aversion, η, equal to 2. We refer readers to Nath et al. (2022) for details on the calculation.

it seems likely that the full mortality risk and mortality partial SCC would be smaller, as people from regions with high damages (e.g., sub-Saharan Africa) may move to regions with low or even negative damages (e.g., Scandinavia, Canada, and Russia). However, both distant and recent history in the United States and around the world underscores that borders are meaningful and there are substantial costs to migration that seem likely to limit the scale of feasible migrations. Indeed, existing empirical evidence of climate-induced migration, based on observable changes in climate to date, is mixed (Carleton and Hsiang 2016).

VIII.B. Humidity

Our estimates do not directly incorporate the role of humidity in historical mortality-temperature relationships nor in projections of future effects. There is growing evidence that humidity influences human health by making it more difficult for the human body to cool itself during hot conditions (e.g., Sherwood and Huber 2010; Barreca 2012). While temperature and humidity are highly correlated over time, they are differentially correlated across space, implying that our measures of heterogeneous mortality-temperature relationships may be influenced by the role of humidity. However, the absence of high-resolution historical humidity data and the highly uncertain projections of humidity under climate change (Sherwood and Fu 2014) make it infeasible to include this heterogeneity in this study's analysis. Emerging work on this topic (Yuan, Stein, and Kopp 2020) is likely to provide opportunities to explore humidity in future research.

VIII.C. Technological Change

The article's projections incorporate advancements in technology that enhance adaptive ability, even though we have not explicitly modeled technological change. In particular, we allow the mortality-temperature response functions to evolve in accordance with rising incomes and temperatures and do not restrict them to stay within the bounds of the current observed distribution of temperature responses. Although our estimates reflect technical advancement as it historically relates to incomes and climate, they do not reflect the seemingly high probability of climate-biased technical change that lowers the relative costs of goods which reduce the health risks of high temperatures. Therefore, the results may overstate the mortality risk of climate change.

IX. Conclusion

This article has outlined a new method that allows for empirical estimation of the global damages of climate change, accounting for the costs and benefits of adaptation, for a single sector of the economy using micro data. We implemented this approach in the context of mortality risks associated with temperature change. Specifically, this study develops a framework for estimating the annual total effect of climate change on mortality risk, both globally and for 24,378 regions that make up the planet. It then uses these estimates to compute a mortality partial SCC, defined as the global marginal WTP to avoid the changes in mortality risk caused by the release of an additional metric ton of CO_2.

There are three noteworthy methodological innovations and key findings. First, we leverage highly resolved data covering roughly half of the world's population to estimate flexible empirical models relating mortality rates to temperature. These regressions uncover a plausibly causal U-shaped relationship where extreme cold and hot temperatures increase mortality rates, especially for those 65 and older. Moreover, this relationship is quite heterogeneous across the planet as both income and long-run climate substantially moderate mortality sensitivity to temperature. Furthermore, when combined with current global data on climate, income, and population, the results imply that the effect of a hot day (35°C/95°F) on mortality in the >64 age group is $\sim$50% larger in regions of the world without available mortality data. This suggests that prior estimates based on data from wealthy economies and temperate climates are likely to understate the true global effects of climate change on human mortality.

Second, we use these regression results along with future projections of climate, income, and population to estimate future climate change–induced mortality risk in terms of fatality rates and its monetized value. We find that under a high-emissions scenario, the projected effect of climate change on mortality will be comparable globally to leading causes of death today, such as cancer and infectious disease (Figure IX). We also estimate large benefits from mitigation, as the end-of-century estimate of the mortality risk of climate change falls from 73 deaths per 100,000 under the high-emissions growth RCP8.5 scenario to 11 per 100,000 under the more moderate RCP4.5 scenario. Importantly, these projected effects include the benefits of adaptation to gradual climate change; estimates that do not account for adaptation overstate the

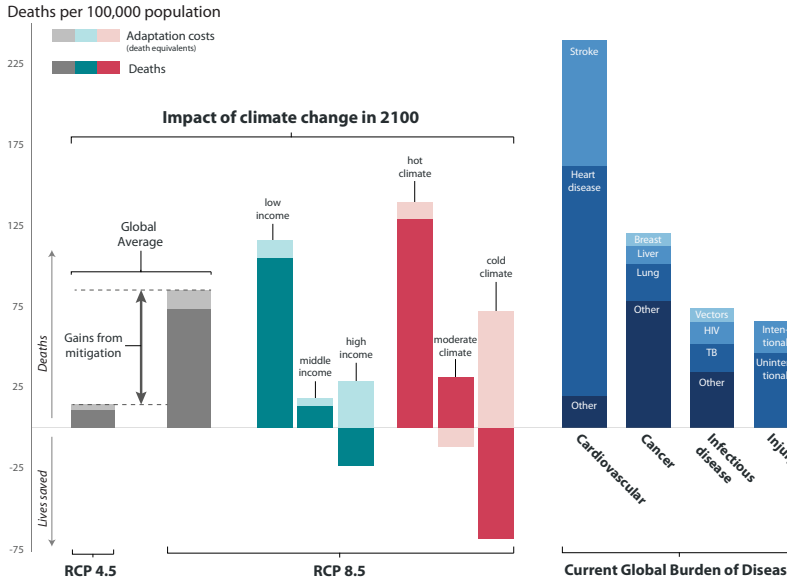

FIGURE IX

The Mortality Effects of Climate Change in 2100 are Comparable to Contemporary Leading Causes of Death

Effects of climate change are calculated for 2100 for socioeconomic scenario SSP3 and include changes in death rates (dark shading) and changes in adaptation costs, measured in death equivalents (light shading). Global averages for RCP 8.5 and RCP 4.5 are shown in the far left, demonstrating the gains from mitigation. Income and average climate groups under RCP8.5 are separated by tercile of the 2015 global distribution across all 24,378 impact regions. Bars on the far right indicate average mortality rates globally in 2018, with values from WHO (2018). Online Appendix Figure F.8 replicates this figure for RCP4.5.

mortality effects of climate change in 2100 by a factor of about three. In addition, we outline and implement a revealed-preference method to infer the costs of these adaptation investments, which amount to, on average, 12 death equivalents per 100,000 by 2100 in the RCP8.5 scenario.

The estimated mortality effects of climate change are distributed unevenly across the world. For example, by 2100 and under a high-emissions scenario, we project that climate change will cause approximately 160 additional deaths per 100,000 annually in Accra, Ghana, but will save approximately 150 lives per 100,000 in Berlin, Germany. Notably, the degree to which the full

mortality risk of climate change is realized through actual deaths, as opposed to costly adaptation, varies widely across space and time. For example, Figure IX shows that today's poor locations tend to bear a larger share of the projected burden in the form of direct mortality effects, while today's rich face large increases in projected adaptation costs.

Third, we use these projections to develop the first empirically grounded estimates of the mortality partial SCC. Using a 2% discount rate and age-varying VSL, the 2020 mortality partial SCC is roughly $36.6 (in 2019 US$) with a high-emissions scenario and $17.1 with a moderate one. There is substantial uncertainty around these estimates, arising both from climate sensitivity and damage function uncertainty. For example, the interquartile ranges of the mortality partial SCC are [−$7.8, $73.0] and [−$24.7, $53.6], under high- and moderate-emissions scenarios, respectively. We find that valuing this uncertainty using standard calibrations of risk aversion increases the mortality partial SCC by about four times.

Overall, the article's findings suggest that previous research has significantly understated climate change damages due to mortality. For instance, we estimate that the full mortality risk of climate change in 2100 amounts to 49% to 135% of total damages across all sectors of the economy according to leading IAMs. Moreover, the mortality partial SCC reported here, under comparable valuation assumptions, is more than 10 times larger than the total health effects embedded in the FUND IAM (Diaz 2014).[41]

We believe that this study has highlighted a key role for systematic empirical analysis in providing a clearer picture of the magnitude of the effects of climate change and how, why, and where they are likely to emerge in the future. It is no longer necessary to rely so heavily on assumptions when estimating the economic costs of climate change. Looking ahead, the article's general approach can be applied to other aspects of the global economy besides mortality risk, and doing so is a promising area for future research.

41. Diaz (2014) computes comparable partial SCC values for FUND ($\delta = 3\%$, "business as usual" emissions) and reports values for three comparable health effects (diarrhea, vector-borne diseases, and cardiopulmonary) that total less than $2 (2019 US$).

University of California, Santa Barbara, and National Bureau of Economic Research, United States
University of Chicago and National Bureau of Economic Research, United States
Rhodium Group, United States
University of Chicago and National Bureau of Economic Research, United States
Rhodium Group, United States
University of California, Berkeley, and National Bureau of Economic Research, United States
University of Chicago, United States
Rutgers University, United States
Rhodium Group, United States
Princeton University, United States
University of Delaware, United States
University of Chicago, United States
World Bank, United States
CompetitionSphere, Belgium
Fudan University, People's Republic of China
Washington and Lee University, United States

Supplementary Material

An Online Appendix for this article can be found at *The Quarterly Journal of Economics* online.

Data Availability

Data and code replicating the tables and figures in this article can be found in Carleton et al. (2022) in the Harvard Dataverse, https://doi.org/10.7910/DVN/FXXLYZ. Replication code is also publicly available at https://github.com/ClimateImpactLab/carleton_mortality_2022 and replication data are publicly hosted at doi.org/10.5281/zenodo.6416119.

References

Alesina, Alberto, and Dani Rodrik, "Distributive Politics and Economic Growth," *Quarterly Journal of Economics*, 109 (1994), 465–490.
Anthoff, David, and Richard S. J. Tol, "The Climate Framework for Uncertainty, Negotiation and Distribution (FUND): Technical Description, Version 3.6," FUND Doc, 2014.
Ashenfelter, Orley, and Michael Greenstone, "Using Mandated Speed Limits to Measure the Value of a Statistical Life," *Journal of Political Economy*, 112 (2004), S226–S267.
Auffhammer, Maximilian, "Climate Adaptive Response Estimation: Short and Long Run Impacts of Climate Change on Residential Electricity and Natural Gas Consumption Using Big Data," NBER Working Paper no. 24397, 2018.

Auffhammer, Maximilian, and Anin Aroonruengsawat, "Simulating the Impacts of Climate Change, Prices and Population on California's Residential Electricity Consumption," *Climatic Change*, 109 (2011), 191–210.
Bailey, Martha J., and Andrew Goodman-Bacon, "The War on Poverty's Experiment in Public Medicine: Community Health Centers and the Mortality of Older Americans," *American Economic Review*, 105 (2015), 1067–1104.
Barreca, Alan I., "Climate Change, Humidity, and Mortality in the United States," *Journal of Environmental Economics and Management*, 63 (2012), 19–34.
Barreca, Alan, Karen Clay, Olivier Deschênes, Michael Greenstone, and Joseph S. Shapiro, "Convergence in Adaptation to Climate Change: Evidence from High Temperatures and Mortality, 1900–2004," *American Economic Review*, 105 (2015), 247–251.
———, "Adapting to Climate Change: The Remarkable Decline in the US Temperature-Mortality Relationship over the Twentieth Century," *Journal of Political Economy*, 124 (2016), 105–159.
Board of Governors of the U.S. Federal Reserve System, "10-Year Treasury Inflation-Indexed Security, Constant Maturity [DFII10]," Technical report, FRED, Federal Reserve Bank of St. Louis, 2020.
Bright, E. A., P. R. Coleman, A. N. Rose, and M. L. Urban, "LandScan 2011." [data set], 2012, web.ornl.gov/sci/landscan/index.shtml.
Burgess, Robin, Olivier Deschênes, Dave Donaldson, and Michael Greenstone, "The Unequal Effects of Weather and Climate Change: Evidence from Mortality in India," LSE Working Paper, 2017.
Burke, Marshall, John Dykema, David B. Lobell, Edward Miguel, and Shanker Satyanath, "Incorporating Climate Uncertainty into Estimates of Climate Change Impacts," *Review of Economics and Statistics*, 97 (2015), 461–471.
Burke, Marshall, Solomon M. Hsiang, and Edward Miguel, "Global Non-Linear Effect of Temperature on Economic Production," *Nature*, 527 (2015), 235–239.
Butler, Ethan E., and Peter Huybers, "Adaptation of US Maize to Temperature Variations," *Nature Climate Change*, 3 (2013), 68–72.
Carleton, Tamma, and Michael Greenstone, "Updating the United States Government's Social Cost of Carbon," *Review of Environmental Economics and Policy* (forthcoming).
Carleton, Tamma A., and Solomon M. Hsiang, "Social and Economic Impacts of Climate," *Science*, 353 (2016), aad9837.
Carleton, Tamma, Amir Jina, Michael Delgado, Michael Greenstone, Trevor Houser, Solomon Hsiang, Andrew Hultgren, and Robert E. Kopp et al., "Replication Data for: 'Valuing the Global Mortality Consequences of Climate Change Accounting for Adaptation Costs and Benefits'," (2022), Harvard Dataverse, https://doi.org/10.7910/DVN/FXXLYZ.
Center for Systemic Peace, "Polity5: Political Regime Characteristics and Transitions 1800–2018," Center for Systemic Peace, 2020.
Davis, Lucas W., and Paul J. Gertler, "Contribution of Air Conditioning Adoption to Future Energy use Under Global Warming," *Proceedings of the National Academy of Sciences*, 112 (2015), 5962–5967.
Dellink, Rob, Jean Chateau, Elisa Lanzi, and Bertrand Magné, "Long-Term Economic Growth Projections in the Shared Socioeconomic Pathways," *Global Environmental Change*, 42 (2015), 200–214.
Deschênes, Olivier, "Temperature Variability and Mortality: Evidence from 16 Asian Countries," *Asian Development Review*, 35 (2018), 1–30.
Deschênes, Olivier, and Michael Greenstone, "The Economic Impacts of Climate Change: Evidence from Agricultural output and Random fluctuations in Weather," *American Economic Review*, 97 (2007), 354–385.
———, "Climate Change, Mortality, and Adaptation: Evidence from Annual Fluctuations in Weather in the US," *American Economic Journal: Applied Economics*, 3 (2011), 152–185.
Deschênes, Olivier, and Enrico Moretti, "Extreme Weather Events, Mortality, and Migration," *Review of Economics and Statistics*, 91 (2009), 659–681.

Diaz, Delavane, "Evaluating the Key Drivers of the US Government's Social Cost of Carbon: A Model Diagnostic and Inter-Comparison Study of Climate Impacts in DICE, FUND, and PAGE," SSRN Working Paper, 2014, http://dx.doi.org/10.2139/ssrn.2655889.
Eurostat, *Europe in Figures: Eurostat Yearbook 2013* (Luxembourg: Publications Office of the European Union, 2013).
Fetzer, Thiemo, "Can Workfare Programs Moderate Conflict? Evidence from India," *Journal of the European Economics Association*, 18 (2020), 3337–3375.
Gasparrini, Antonio, Yuming Guo, Francesco Sera, Maria Ana Vicedo-Cabrera, Veronika Huber, Shilu Tong, Micheline de Sousa Zanotti Stagliorio Coelho, and Paulo Hilario Nascimento Saldiva, et al., "Projections of Temperature-Related Excess Mortality under Climate Change Scenarios," *Lancet Planetary Health*, 1 (2017), e360–e367.
Gennaioli, Nicola, Rafael La Porta, Florencio Lopez De Silanes, and Andrei Shleifer, "Growth in Regions," *Journal of Economic Growth*, 19 (2014), 259–309.
Glaeser, Edward L., Rafael La Porta, Florencio Lopez-de Silanes, and Andrei Shleifer, "Do Institutions Cause Growth?," *Journal of Economic Growth*, 9 (2004), 271–303.
Graff Zivin, Joshua, and Matthew Neidell, "Temperature and the Allocation of Time: Implications for Climate Change," *Journal of Labor Economics*, 32 (2014), 1–26.
Greenstone, Michael, Elizabeth Kopits, and Ann Wolverton, "Developing a Social Cost of Carbon for US Regulatory Analysis: A Methodology and Interpretation," *Review of Environmental Economics and Policy*, 7 (2013), 23–46.
Heutel, Garth, Nolan H. Miller, and David Molitor, "Adaptation and the Mortality Effects of Temperature across US Climate Regions," NBER Working Paper no. 23271, 2017.
Houser, Trevor, Solomon Hsiang, Robert Kopp, and Kate Larsen, *Economic Risks of Climate Change: An American Prospectus* (New York: Columbia University Press, 2015).
Hsiang, Solomon, "Visually-Weighted Regression," 2013, available at SSRN, http://doi.org/10.2139/ssrn.2265501.
———, "Climate Econometrics," *Annual Review of Resource Economics*, 8 (2016), 43–75.
Hsiang, Solomon, Robert Kopp, Amir Jina, James Rising, Michael Delgado, Shashank Mohan, D. J. Rasmussen, and Robert Muir-Wood et al., "Estimating Economic Damage from Climate Change in the United States," *Science*, 356 (2017), 1362–1369.
Hsiang, Solomon M., and Amir S. Jina, The Causal Effect of Environmental Catastrophe on Long-Run Economic Growth: Evidence from 6,700 Cyclones; NBER Working Paper no. 20352, 2014.
Hsiang, Solomon M., Kyle C. Meng, and Mark A. Cane, "Civil Conflicts Are Associated with the Global Climate," *Nature*, 476 (2011), 438.
Hsiang, Solomon M., and Daiju Narita, "Adaptation to Cyclone Risk: Evidence from the Global Cross-Section," *Climate Change Economics*, 3 (2012), 1250011.
IIASA Energy Program, "SSP Database, Version 1.1" [data set], NBER, 2016.
Interagency Working Group on Social Cost of Carbon, "Social Cost of Carbon for Regulatory Impact Analysis - Under Executive Order 12866," Technical report, 2010.
Interagency Working Group on Social Cost of Greenhouse Gases, "Technical Support Document: Technical Update of the Social Cost of Carbon for Regulatory Impact Analysis," Technical report, 2016.
Isen, Adam, Maya Rossin-Slater, and Reed Walker, "Relationship between Season of Birth, Temperature Exposure, and Later Life Wellbeing," *Proceedings of the National Academy of Sciences*, 114 (2017), 13447–13452.
Jones, Charles I., and Peter J. Klenow, "Beyond GDP? Welfare across Countries and Time," *American Economic Review*, 106 (2016), 2426–57.

Kahn, Matthew E., "The Death Toll from Natural Disasters: the Role of Income, Geography, and Institutions," *Review of Economics and Statistics*, 87 (2005), 271–284.
Kelly, David L., Charles D. Kolstad, and Glenn T. Mitchell, "Adjustment Costs from Environmental Change," *Journal of Environmental Economics and Management*, 50 (2005), 468–495.
Kopp, Robert E., and Bryan K. Mignone, "The US Government's Social cost of Carbon Estimates after their First Two Years: Pathways for Improvement," *Economics*, 6 (2012), 1–41.
La Porta, Rafael, and Andrei Shleifer, "Informality and Development," *Journal of Economic Perspectives*, 28 (2014), 109–126.
Lemoine, Derek, "Estimating the Consequences of Climate Change from Variation in Weather," NBER Working Paper no. 25008, 2018.
Lenssen, N., G. Schmidt, J. Hansen, M. Menne, A. Persin, R. Ruedy, and D. Zyss, "Improvements in the GISTEMP uncertainty model," *Journal of Geophysical Research: Atmospheres*, 124 (2019), 6307–6326.
Matsuura, Kenji, and Cort Willmott, "Terrestrial Air Temperature and Precipitation: 1900–2006 Gridded Monthly Time Series, Version 1.01," University of Delaware 2007.
Mendelsohn, Robert, William D. Nordhaus, and Daigee Shaw, "The Impact of Global Warming on Agriculture: A Ricardian Analysis," *American Economic Review*, 84 (1994), 753–771.
Millar, Richard J., Zebedee R. Nicholls, Pierre Friedlingstein, and Myles R. Allen, "A Modified Impulse-Response Representation of the Global Near-Surface Air Temperature and Atmospheric Concentration Response to Carbon Dioxide Emissions," *Atmospheric Chemistry and Physics*, 17 (2017), 7213–7228.
Moore, Frances C., and David B. Lobell, "Adaptation Potential of European Agriculture in Response to Climate Change," *Nature Climate Change*, 4 (2014), 610.
Murphy, Kevin M., and Robert H. Topel, "The Value of Health and Longevity," *Journal of Political Economy*, 114 (2006), 871–904.
Nath, Ishan, Tamma Carleton, Michael Greenstone, Trevor Houser, Solomon Hsiang, Andrew Hultgren, Amir Jina, and Robert E. Kopp et al., "The Welfare Economics of a Data-Driven Social Cost of Carbon," University of Chicago Working Paper, 2022.
Nordhaus, William D., "An Optimal Transition Path for Controlling Greenhouse Gases," *Science*, 258 (1992), 1315–1319.
Nordhaus, William D., and Zili Yang, "A Regional Dynamic General-Equilibrium Model of Alternative Climate-Change Strategies," *American Economic Review*, 86 (1996), 741–765.
Organization of Economic Cooperaton and Development, "OECD.Stat," OECD, 2020.
Rasmussen, D. J., Malte Meinshausen, and Robert E. Kopp, "Probability-Weighted Ensembles of U.S. County-Level Climate Projections for Climate Risk Analysis," *Journal of Applied Meteorology and Climatology*, 55 (2016), 2301–2322.
Riahi, Keywan, Detlef P. Van Vuuren, Elmar Kriegler, Jae Edmonds, Brian C. O'neill, Shinichiro Fujimori, Nico Bauer, and Katherine Calvin et al., "The Shared Socioeconomic Pathways and Their Energy, Land Use, and Greenhouse Gas Emissions Implications: An Overview," *Global Environmental Change*, 42 (2017), 153–168.
Rode, Ashwin, Tamma Carleton, Michael Delgado, Michael Greenstone, Trevor Houser, Solomon Hsiang, Andrew Hultgren, and Amir Jina et al., "Estimating a Social Cost of Carbon for Global Energy Consumption," *Nature*, 598 (2021), 308–314.
Rohde, Robert, Richard Muller, Robert Jacobsen, Saul Perlmutter, Arthur Rosenfeld, Jonathan Wurtele, J. Curry, and Charlotte Wickham et al., "Berkeley Earth Temperature Averaging Process," *Geoinformatics and Geostatistics: An Overview*, 1 (2013), 1–13.

Schlenker, Wolfram, and Michael J. Roberts, "Nonlinear Temperature Effects Indicate Severe Damages to US Crop Yields under Climate Change," *Proceedings of the National Academy of Sciences*, 106 (2009), 15594–15598.
Schlenker, Wolfram, Michael J. Roberts, and David B. Lobell, "US Maize Adaptability," *Nature Climate Change*, 3 (2013), 690–691.
Sheffield, Justin, Gopi Goteti, and Eric F. Wood, "Development of a 50-Year High-Resolution Global Dataset of Meteorological Forcings for Land Surface Modeling," *Journal of Climate*, 19 (2006), 3088–3111.
Sherwood, Steven, and Qiang Fu, "A Drier Future?," *Science*, 343 (2014), 737–739.
Sherwood, Steven C., and Matthew Huber, "An Adaptability Limit to Climate Change due to Heat Stress," *Proceedings of the National Academy of Sciences*, 107 (2010), 9552–9555.
Solon, Gary, Steven J. Haider, and Jeffrey M. Wooldridge, "What Are We Weighting For?," *Journal of Human Resources*, 50 (2015), 301–316.
Stern, Nicholas, *The Economics of Climate Change: The Stern Review* (Cambridge: Cambridge University Press, 2006).
Tebaldi, Claudia, and Reto Knutti, "The Use of the Multi-Model Ensemble in Probabilistic Climate Projections," *Philosophical Transactions of the Royal Society of London A: Mathematical, Physical and Engineering Sciences*, 365 (2007), 2053–2075.
Thaler, Richard, and Sherwin Rosen, "The Value of Saving a Life: Evidence from the Labor Market." In *Household Production and Consumption,* Nesteor E. Terlekyj, ed. (Cambridge, MA: NBER, 1976), 265–302.
Thomson, Allison M., Katherine V. Calvin, Steven J. Smith, G. Page Kyle, April Volke, Pralit Patel, Sabrina Delgado-Arias, and Ben Bond-Lamberty et al., "RCP4.5: A Pathway for Stabilization of Radiative Forcing by 2100," *Climatic Change*, 109 (2011), 77.
Thrasher, Bridget, Edwin P. Maurer, C. McKellar, and P. B. Duffy, "Technical Note: Bias Correcting Climate Model Simulated Daily Temperature Extremes with Quantile Mapping," *Hydrology and Earth System Sciences*, 16 (2012), 3309–3314.
Tol, Richard S. J., "On the Optimal Control of Carbon Dioxide Emissions: An Application of FUND," *Environmental Modeling & Assessment*, 2 (1997), 151–163.
Traeger, Christian P., "Why Uncertainty Matters: Discounting under Intertemporal Risk Aversion and Ambiguity," *Economic Theory*, 56 (2014), 627–664.
U.S. Environmental Protection Agency, "Recommended Income Elasticity and Income Growth Estimates: Technical Memorandum," U.S. Environmental Protection Agency Office of Air and Radiation and Office of Policy Technical Report, 2016a.
———, "Valuing Mortality Risk Reductions for Policy: A Meta-Analytic Approach," U.S. Environmental Protection Agency Office of Policy, National Center for Environmental Economics Technical report, 2016b.
Van Vuuren, Detlef P., Jae Edmonds, Mikiko Kainuma, Keywan Riahi, Allison Thomson, Kathy Hibbard, George C. Hurtt, and Tom Kram et al., "The Representative Concentration Pathways: An Overview," *Climatic Change*, 109 (2011), 5.
Viscusi, W. Kip, "The Role of Publication Selection bias in Estimates of the Value of a Statistical Life," *American Journal of Health Economics*, 1 2015, https://doi.org/10.1162/ajhe_a_00002.
WHO, "Global Health Estimates 2016: Deaths by Cause, Age, Sex, by Country and by Region, 2000–2016," World Health Organization Technical report, 2018.
World Bank, "World Development Indicators," World Bank, 2020.
World Inequality Lab, "World Inequality Database," World Inequality Lab, 2020.
Yuan, Jiacan, Michael L. Stein, and Robert E. Kopp, "The Evolving Distribution of Relative Humidity Conditional upon Daily Maximum Temperature in a Warming Climate," *Journal of Geophysical Research: Atmospheres*, 125 (2020), e2019JD032100.

CALL FOR NOMINATIONS

$300,000 Nemmers Prize in Economics

Northwestern University invites nominations for the Erwin Plein Nemmers Prize in Economics, to be awarded during the 2026–27 academic year. The prize pays the recipient $300,000. Recipients of the Nemmers Prize present lectures, participate in department seminars, and engage with Northwestern faculty and students in other scholarly activities.

Details about the prize and the nomination process can be found at **nemmers.northwestern.edu**. Candidacy for the Nemmers Prize is open to those with careers of outstanding achievement in their disciplines as demonstrated by major contributions to new knowledge or the development of significant new modes of analysis.Individuals of all nationalities and institutional affiliations are eligible except current or recent members of the Northwestern University faculty and past recipients of the Nemmers or Nobel Prize. **Nominations will be accepted until January 14, 2026.**

The Nemmers prizes are made possible by a generous gift to Northwestern University by the late Erwin Esser Nemmers and the late Frederic Esser Nemmers.

Northwestern

Nemmers Prizes • Office of the Provost • Northwestern University • Evanston, Illinois 60208
nemmers.northwestern.edu